Introduction to the SiPM working principle

4. Detector Workshop

of the

Helmholtz Alliance "Physics at the Terascale"

Markus Merschmeyer
Physics Institute IIIA, RWTH Aachen University

SiPMs...

...usually are arrays of Geiger-mode avalanche photodiodes with passive quenching made of doped silicon...

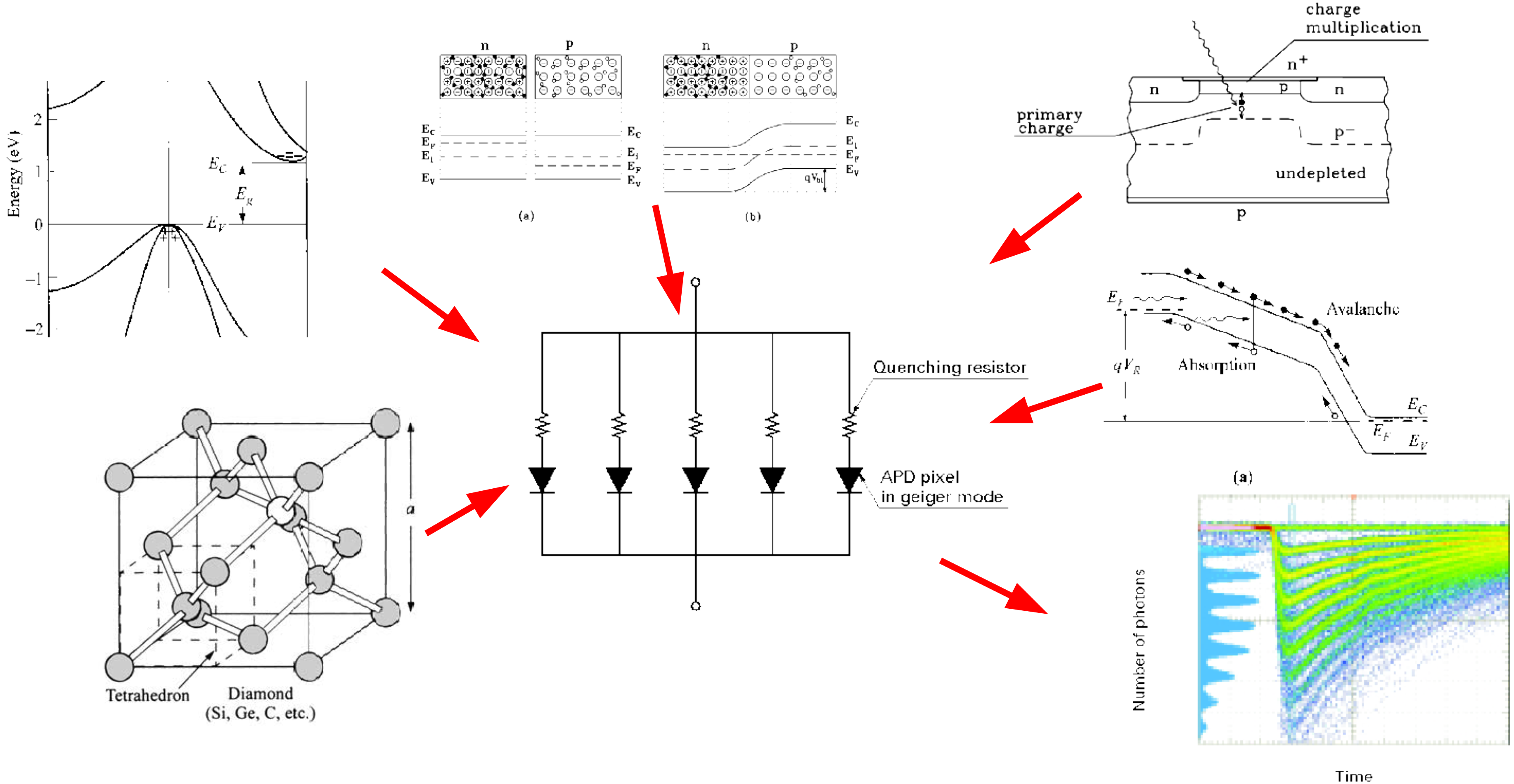

Overview

I. Semiconductor Basics

II. p-n Junctions

III. Photodetectors

IV. Silicon Photomultipliers

V. Special Topics

Literature

- S.M. Sze, K.K. Ng: „Physics of Semiconductor Devices“, Wiley, 2007
- G. Lutz: „Semiconductor Radiation Detectors“, Springer, 1999
- H. Göbel: „Einführung in die Halbleiter-Schaltungstechnik“, Springer, 2008
- presentations by Y. Musienko, and various papers...

RWTH AACHEN UNIVERSITY

I. Semiconductor Basics

Structure of Semiconductors

S.M. Sze, K.K. Ng, Wiley, 2007

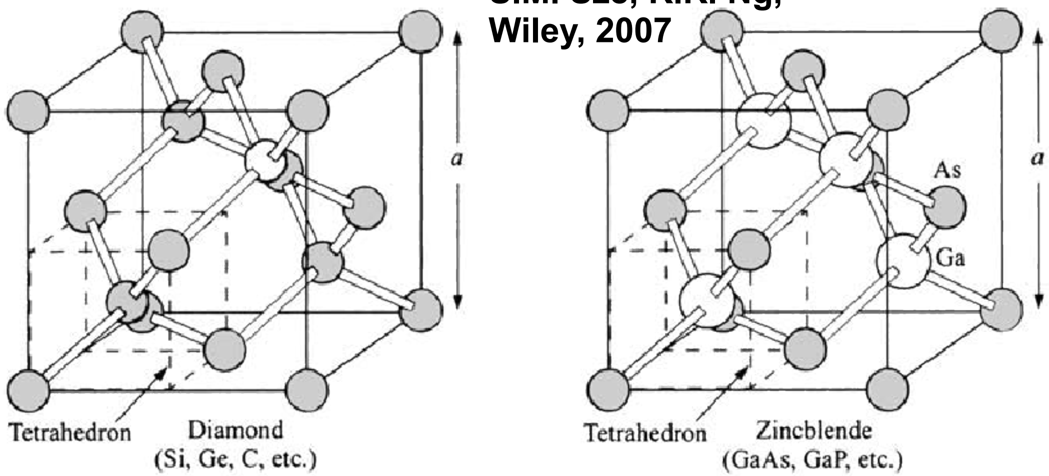

- primitive cell has diamond structure
  - two intersecting fcc lattices
  - tetrahedral covalent bonds (Si: [Ne] $3s^2\ 3p^2$: [Ne] $3[sp^3]^4$)
- inner shells are full and do not contribute to the binding

- intrinsic properties

(T = 300K)	**Si**	**GaAs**
a / Å	5.4	5.7
ε_{pair} / eV	3.6	4.4
drift mobility		
electrons / cm^2/Vs	~ 1450	~ 8800
holes / cm^2/Vs	~ 500	~ 320
saturation velocity		
electrons / cm/s	1×10^7	
holes / cm/s	8.4×10^6	10^7

- semiconductor devices are built on the surface
  → orientation of crystal planes

Reciprocal Lattice

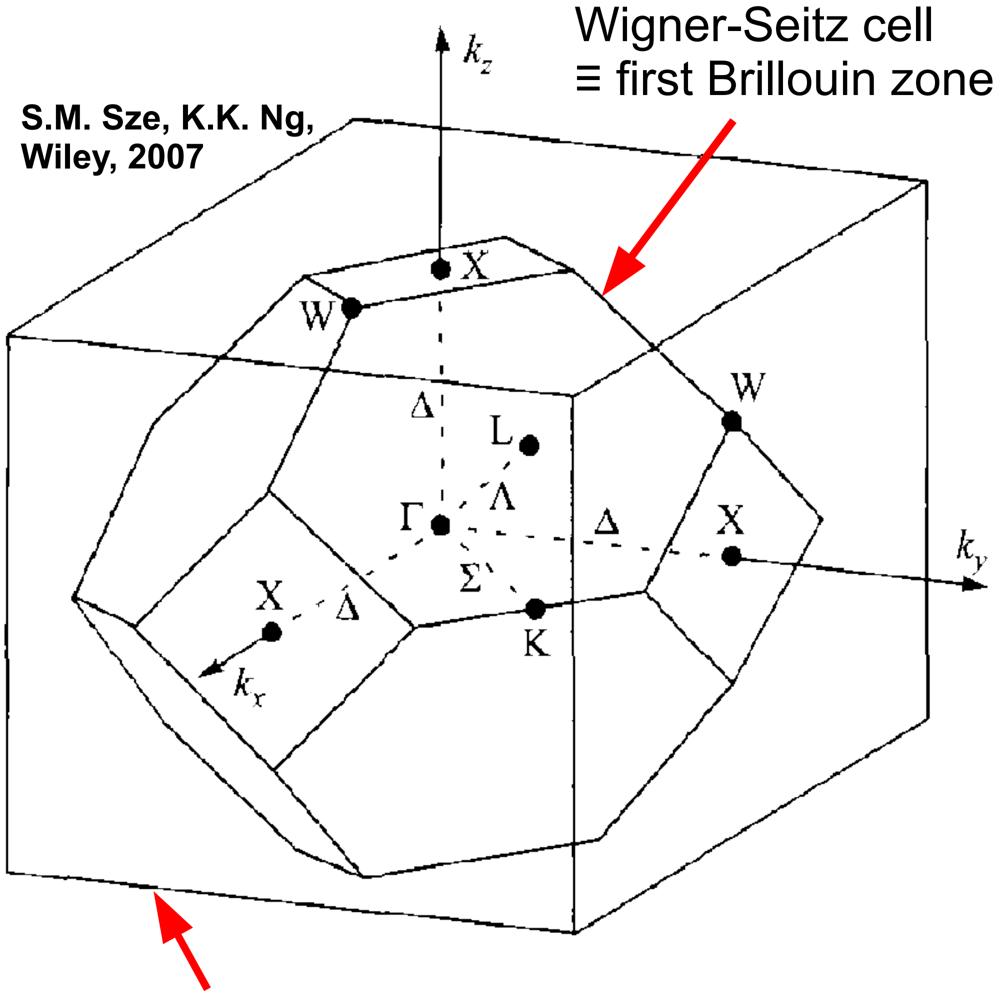

primitive cell of a **bcc** reciprocal lattice for a direct **fcc** lattice

- basis vectors of primitive cell

$$\vec{a}, \vec{b}, \vec{c} \quad \Rightarrow \quad \vec{R} = m\vec{a} + n\vec{b} + p\vec{c}$$

- basis vectors of reciprocal lattice

$$\vec{a}^* = 2\pi \frac{\vec{b}\times\vec{c}}{\vec{a}\cdot\vec{b}\times\vec{c}}, \quad \ldots$$

- helps to visualize energy band structures along main directions of the crystal
  - points : *Γ* (0,0,0), *X*, *L*, *K*
  - directions: <1,0,0>: *Δ*, <1,1,1>: *Λ*, <1,1,0>: *Σ*
- orientation of standard Si wafers <1,0,0> or <1,1,1>

Energy Bands

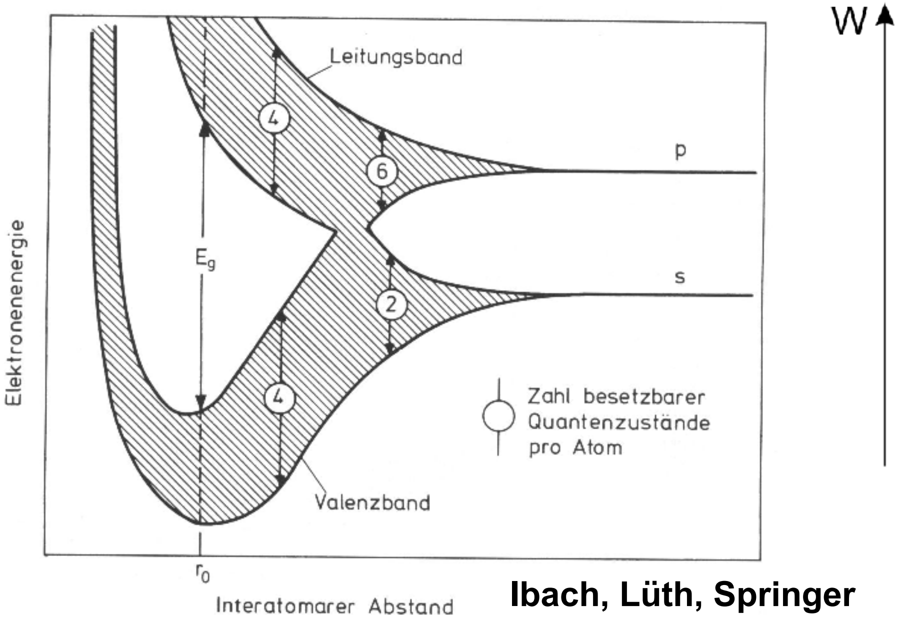

Ibach, Lüth, Springer

H. Göbel, Springer, 2008

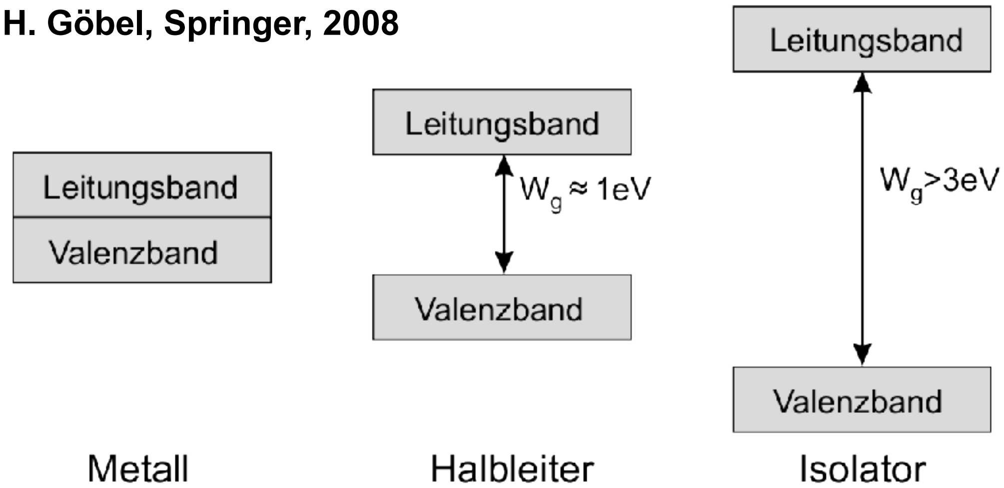

- atoms have discrete energy levels
- evolve into energy bands when
  - distance of atoms decreases
  - number of atoms increases

→ valence band and conduction band with possible energy gap

- width of energy gap determines nature of the material
- conduction band empty at T=0K
- at T>0K electrons can get into the conduction band by thermal excitation

Energy Bands and Band Gap

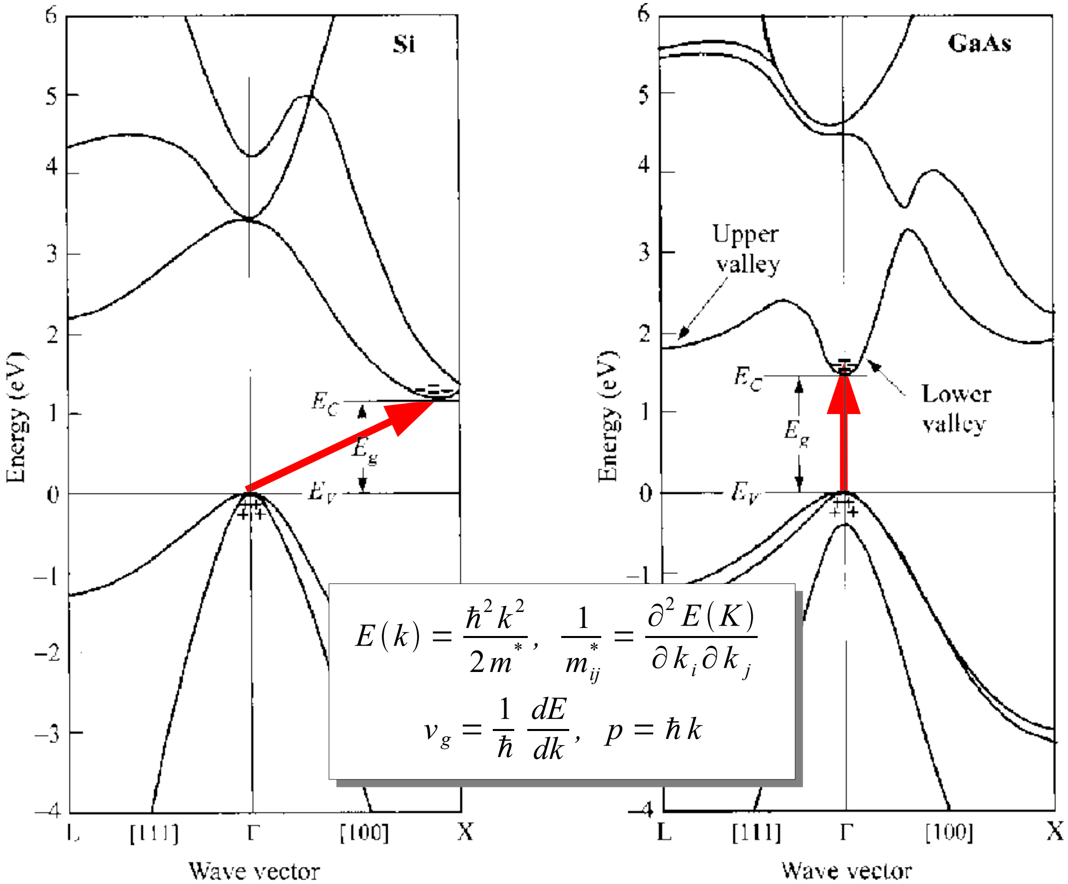

$$E(k) = \frac{\hbar^2 k^2}{2m^*}, \quad \frac{1}{m^*_{ij}} = \frac{\partial^2 E(K)}{\partial k_i \partial k_j}$$

$$v_g = \frac{1}{\hbar}\frac{dE}{dk}, \quad p = \hbar k$$

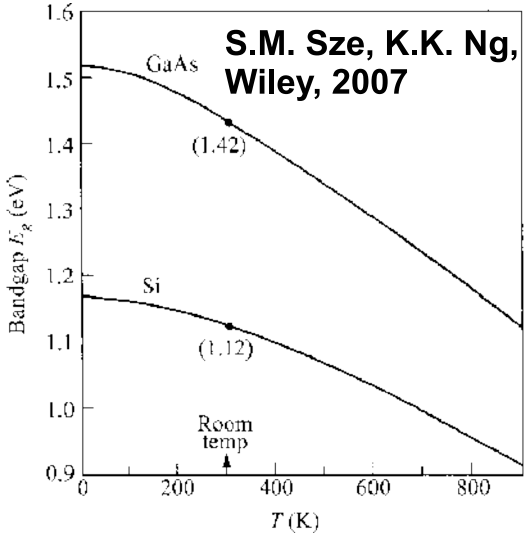

S.M. Sze, K.K. Ng, Wiley, 2007

	$E_g(0)$ (eV)	α (eV/K)	β (K)
GaAs	1.519	5.4×10^{-4}	204
Si	1.169	4.9×10^{-4}	655

$$E_g(T) = E_g(0) - \frac{\alpha T^2}{T+\beta}$$

- width of energy gap
  - decreases with temperature
  - reduces in highly doped materials

- complicated band structure: subbands (can be degenerate)
- indirect (Si) vs. direct (GaAs) semiconductors: E_C(min) shifted w.r.t Γ

Doping

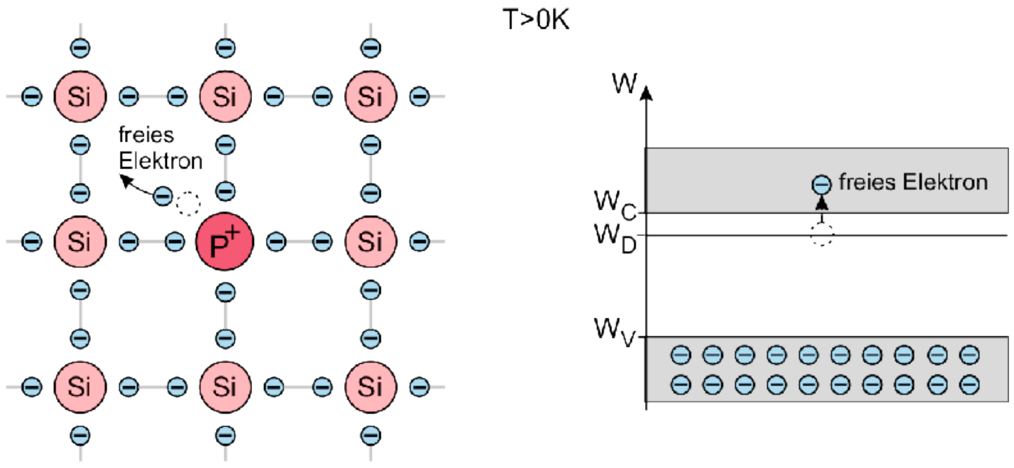

H. Göbel, Springer, 2008

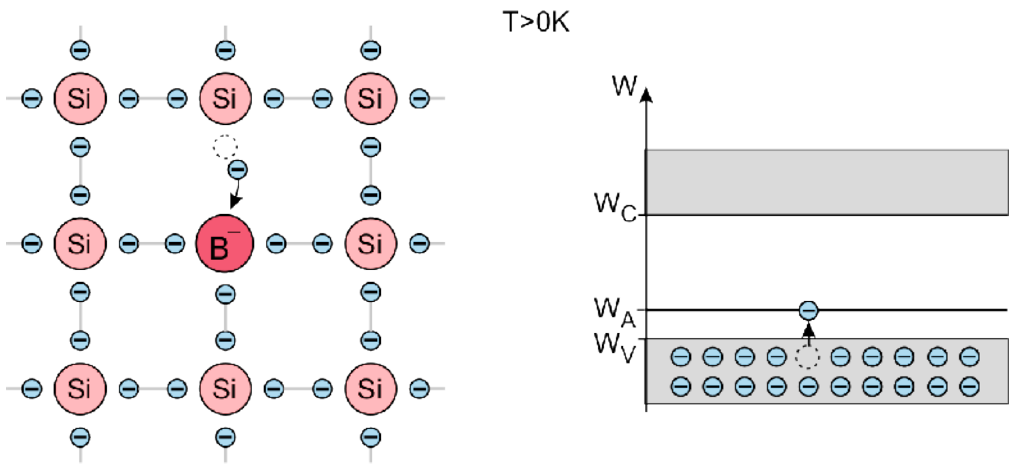

- doping introduces energy levels inside the energy gap
- impurity concentration
  - N_D, N_A ~ $10^{12} - 10^{18}$ cm^{-3}
- dopants for silicon
  - donors: N, **P**, As, Sb, Bi (Gr. V)
    → donor levels: E_C - O(50meV)
  - acceptors: **B**, Al, Ga, In, Tl (Gr. III)
    → acceptor levels: E_V + O(50meV)
- ionization energies comparable to *kT* (~26 meV) → easy thermal excitation, full ionization at 300K

Fermi Level

- number of carriers in conduction band → integrate of number of states *N(E)* and occupancy *F(E)*

$$n = \int_{E_C}^{\infty} N(E) F(E)\, dE$$

- calculation of carrier concentrations requires knowledge of Fermi energy
- electrons

$$n = N_C \exp\left(-\frac{E_C - E_F}{kT}\right), \qquad N_C = 2\left(\frac{2\pi m_{de} kT}{h^2}\right)^{3/2} M_C$$

- holes

$$p = N_V \exp\left(-\frac{E_F - E_V}{kT}\right), \qquad N_V = 2\left(\frac{2\pi m_{dh} kT}{h^2}\right)^{3/2}$$

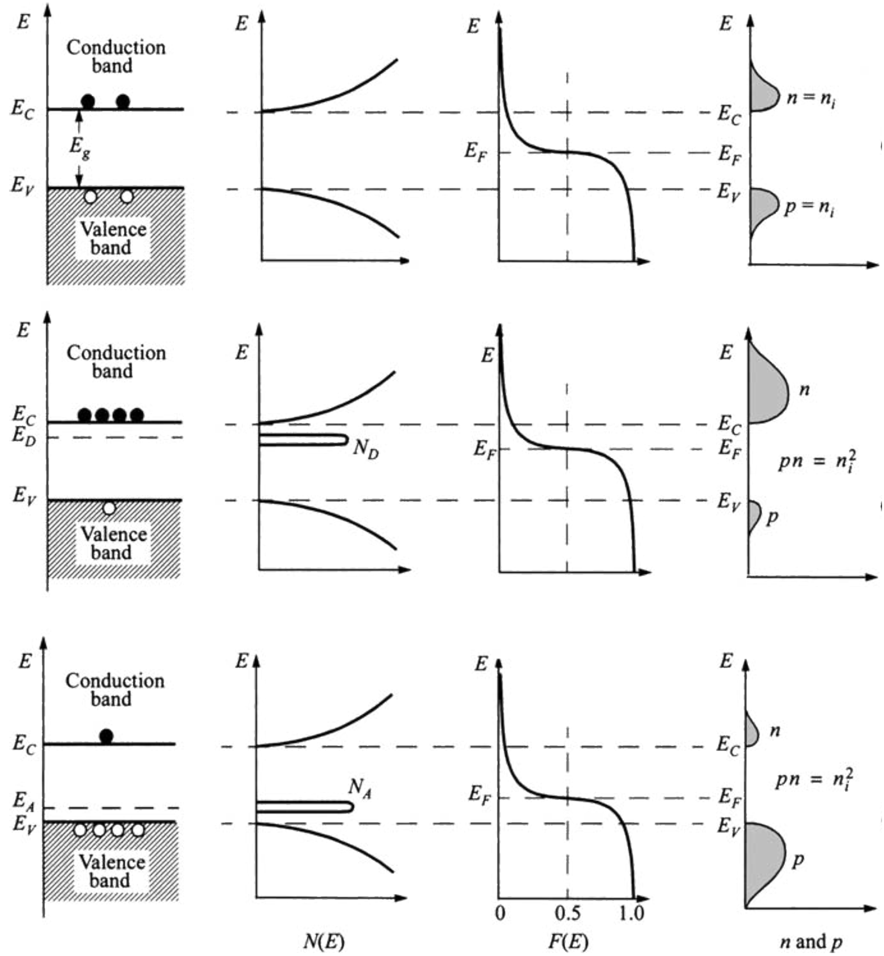

S.M. Sze, K.K. Ng, Wiley, 2007

Intrinsic Charge Carriers

T>0K

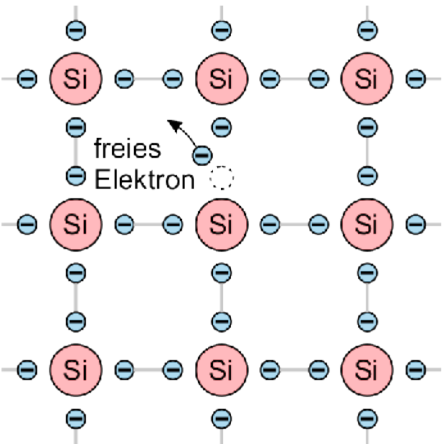

H. Göbel, Springer, 2008

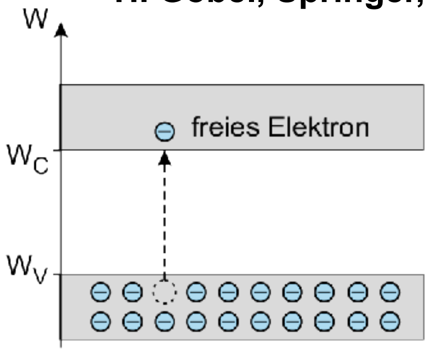

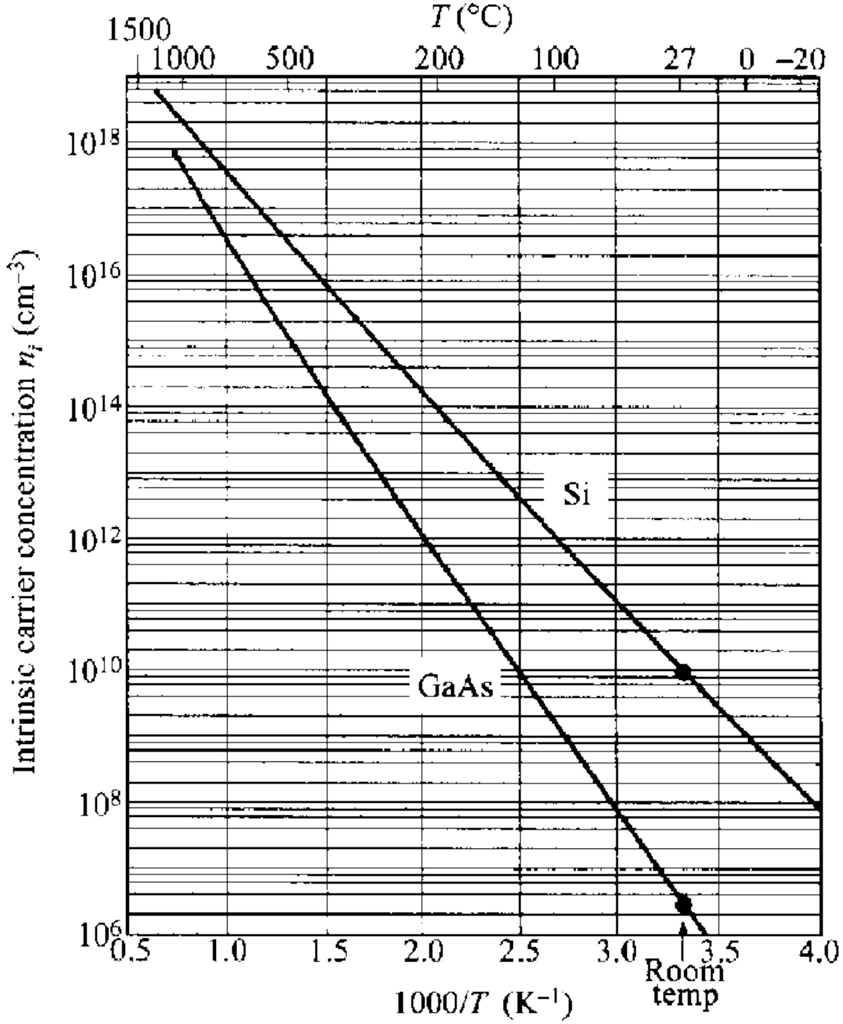

S.M. Sze, K.K. Ng, Wiley, 2007

- thermal excitation in undoped silicon → intrinsic charge carrier density n_i

$$E_F = E_i = \frac{E_C + E_V}{2} + \frac{kT}{2} \ln\left(\frac{N_V}{N_C}\right)$$

yields

$$n_i = N_C \exp\left(-\frac{E_C - E_i}{kT}\right) = \sqrt{N_C N_V} \exp\left(-\frac{E_G}{2\mathrm{kT}}\right)$$

Intrinsic Charge Carriers

- strong temperature dependence of intrinsic carrier density
  - ~ factor 10 between room temperature and 0°C
  - Si is an isolator at liquid nitrogen temperatures
- width of band gap (Si vs. GaAs) plays an additional role

$$\frac{n_i(T)}{n_i(300\mathrm{K})} = \left(\frac{T}{300}\right)^{3/2} \cdot \frac{\exp\left(-\frac{E_G(T)}{2\mathrm{kT}}\right)}{\exp\left(-\frac{E_G(300\mathrm{K})}{2\mathrm{k}\cdot 300}\right)}$$

	Si	GaAs
$E_G(300\mathrm{K})$ / eV	1.12	1.42
$n_i(300\mathrm{K})$ / cm^{-3}	1.45×10^{10}	1.79×10^{6}
$n_i(273\mathrm{K})$ / cm^{-3}	1.27×10^{9}	7.91×10^{4}
$n_i(77\mathrm{K})$ / cm^{-3}	3.80×10^{-20}	9.51×10^{-32}

Carrier Concentration

- concentration of ionized donors and acceptors

$$N_D^+ = \frac{N_D}{1 + g_D \exp\left[(E_F - E_D)/kT\right]}$$

$$N_A^- = \frac{N_A}{1 + g_A \exp\left[(E_A - E_F)/kT\right]}$$

- charge balance

$$n + N_A^- = p + N_D^+$$

$$n \approx \left(\frac{N_D - N_A}{2N_A}\right) N_C \exp\left[-\frac{E_C - E_D}{kT}\right]$$

- mass-action law still applies

$$n_0 = N_D \;\rightarrow\; p_0 = \frac{n_i^2}{N_D} \qquad p_0 = N_A \;\rightarrow\; n_0 = \frac{n_i^2}{N_A}$$

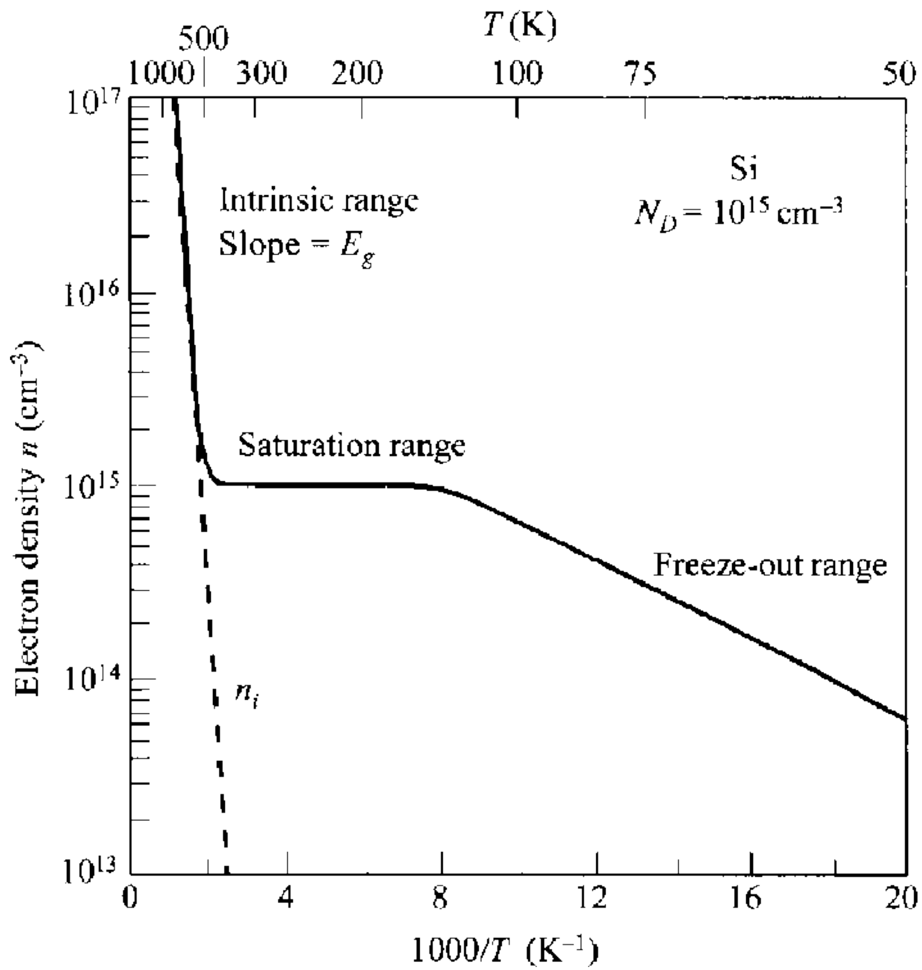

S.M. Sze, K.K. Ng, Wiley, 2007

Carrier Mobility

S.M. Sze, K.K. Ng, Wiley, 2007

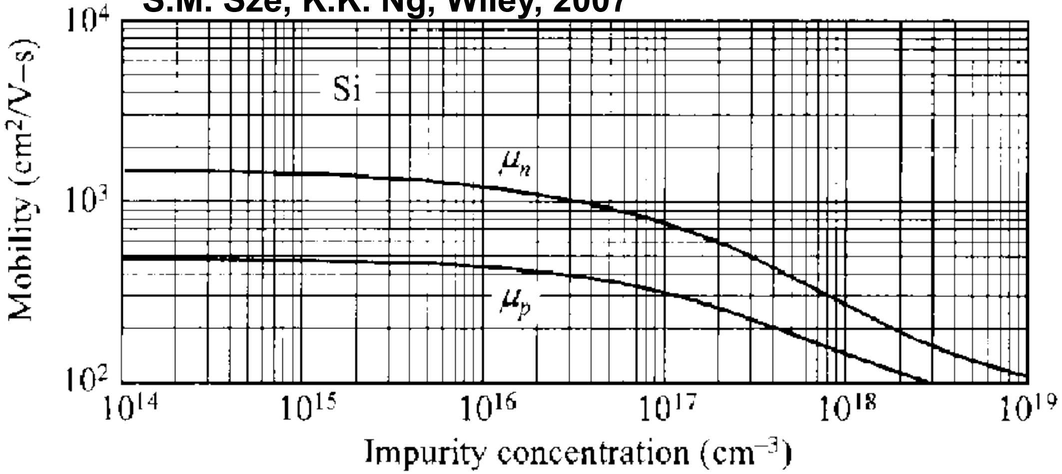

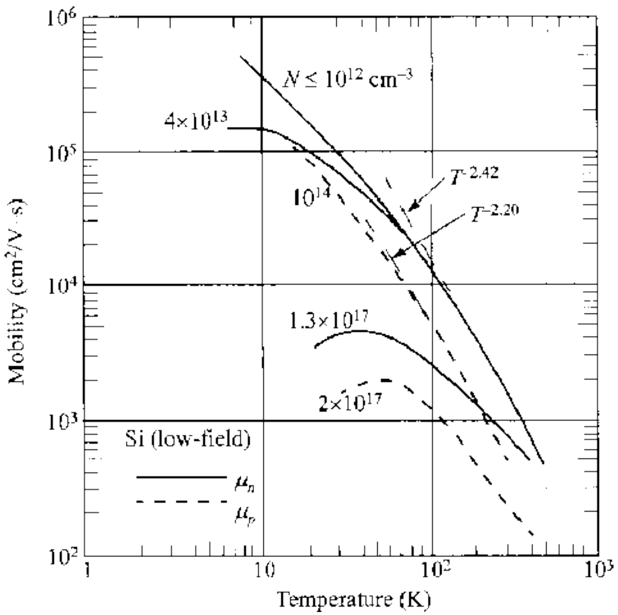

- drift velocity at low fields

$$v_d = \mu\ E$$

- carrier mobility affected by interaction with
  - acoustic phonons

$$\mu_l \propto \frac{1}{m_c^{*\,5/2}\, T^{3/2}}$$

  - ionized impurities

$$\mu_i \propto \frac{T^{3/2}}{N_I\ m^{*1/2}}$$

$$\mu = \left(\frac{1}{\mu_l} + \frac{1}{\mu_i}\right)^{-1}$$

total mobility

→ dependence on

- effective mass
- temperature
- impurity concentration

Carrier Mobility

- charge carriers emit and absorb phonons
- at high electric fields (>10^4V/cm) phonon emission ist more likely → drift velocity saturates at

$$v_s = \sqrt{\frac{8 E_p}{3 \pi m_0}} \approx 10^7 cm/s$$

- (comparable to drift velocities in gas detectors)
- impact ionization only becomes important at field strenghts larger than 10^5 V/cm

S.M. Sze, K.K. Ng, Wiley, 2007

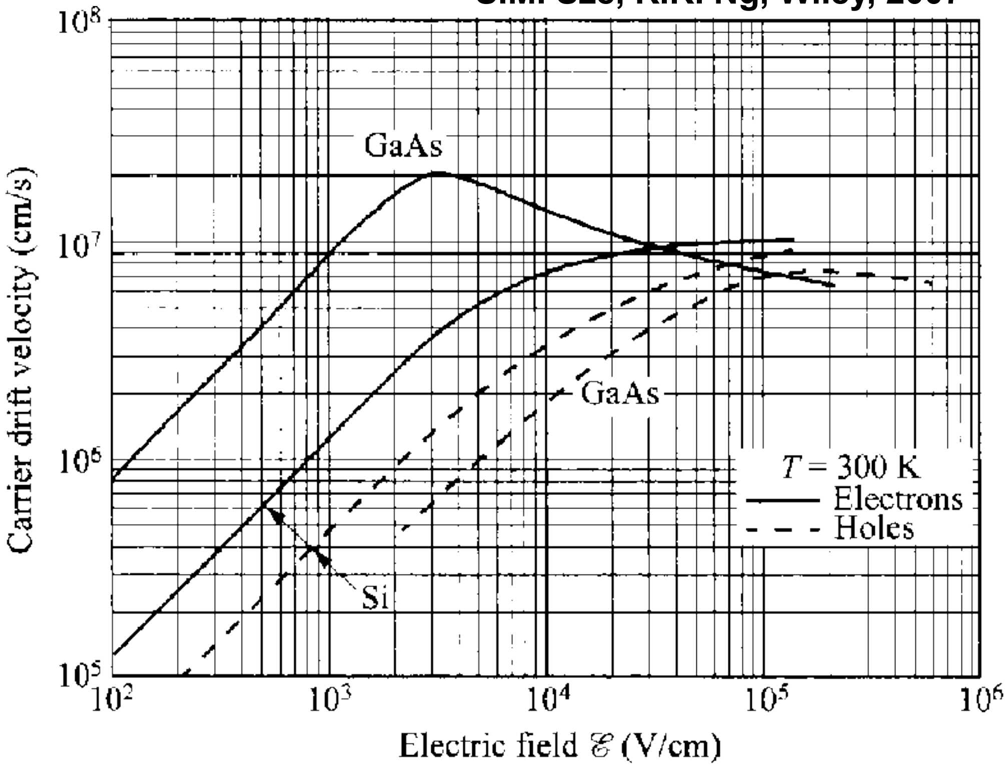

(for high-purity semiconductors)

Impact Ionization

S.M. Sze, K.K. Ng, Wiley, 2007

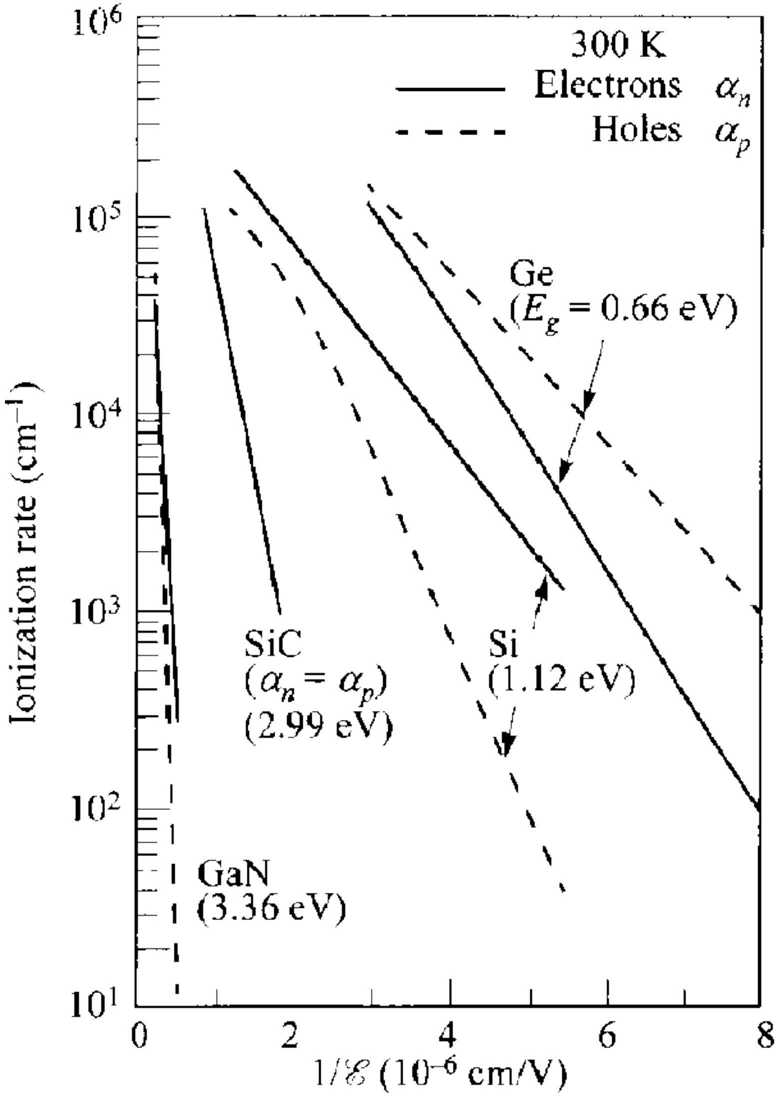

- at sufficiently high fields carriers gain enough energy for secondary ionization
- ionization rate α, e.g. for electrons

$$\alpha_n = \frac{1}{n} \frac{dn}{d(tv_n)} = \frac{1}{nv_n} \frac{dn}{dt}$$

- electron ionization dominates in silicon → device construction (breakdown at lower electric fields)
- generation rate at fixed location

$$\frac{dn}{dt} = \frac{dp}{dt} = \alpha_n n v_n + \alpha_p p v_p$$

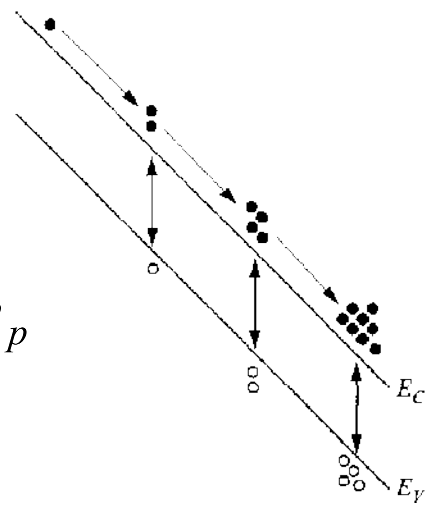

Summary of Part I

- silicon is well suited for building semiconductor photodetectors
  - band gap of 1.12 eV → good absorption for optical photons
  - indirect semiconductor: transition needs additional phonon or larger photon energy
  - can sustain large electric fields → impact ionization, intrinsic amplification

- doping
  - group III elements: „acceptors“, group V elements: „donors“
  - additional energy levels are only O(50meV) above valence band or below conduction band → easy thermal excitation
  - typical impurity concentrations: 10^{12} to 10^{18} cm^{-3}

- drawback: strong temperature dependence of all properties

II. p-n Junction

p-n Junction

- ideal/simple case: abrupt change from donor to acceptor impurities
- semiconductor is electrically neutral in thermal equilibrium

$$N_A W_{Dp} = N_D W_{Dn}$$

- maximum electric field E_m

$$E_m = \frac{qN_D W_{Dn}}{\epsilon_s} = \frac{qN_A W_{Dp}}{\epsilon_s}$$

- built-in (diffusion) potential Ψ_{bi}

$$\Psi_{bi} \approx \frac{kT}{q} \ln\left(\frac{N_D N_A}{n_i^2}\right)$$

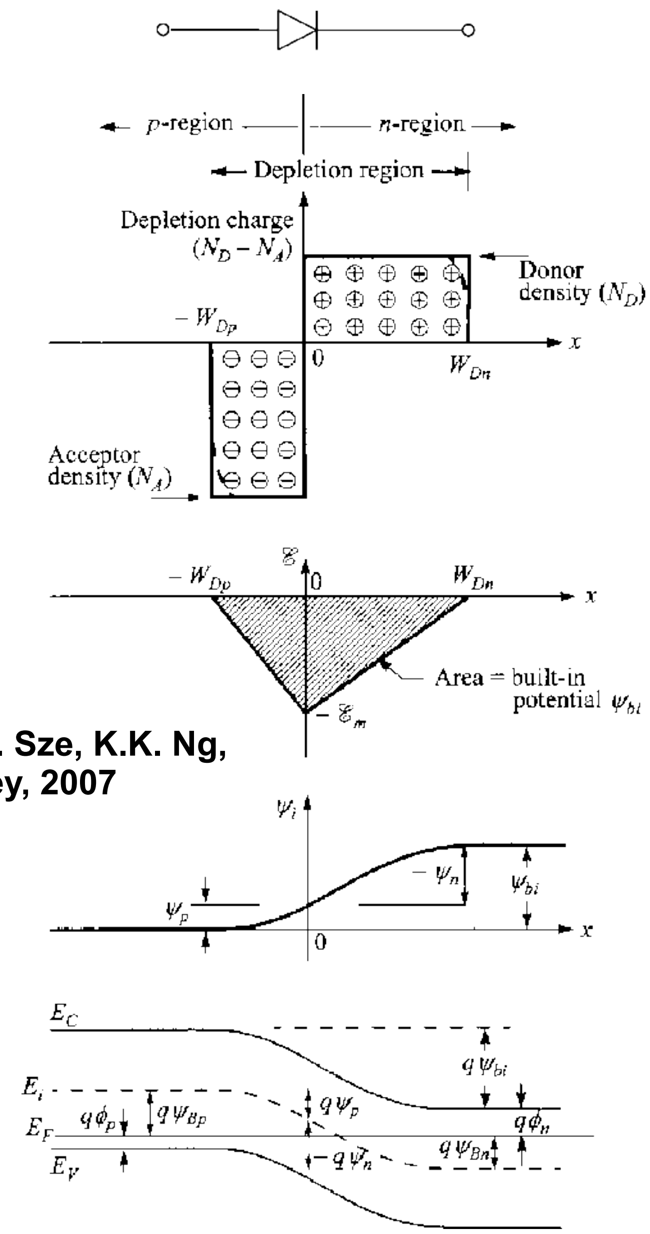

S.M. Sze, K.K. Ng, Wiley, 2007

Depletion Zone

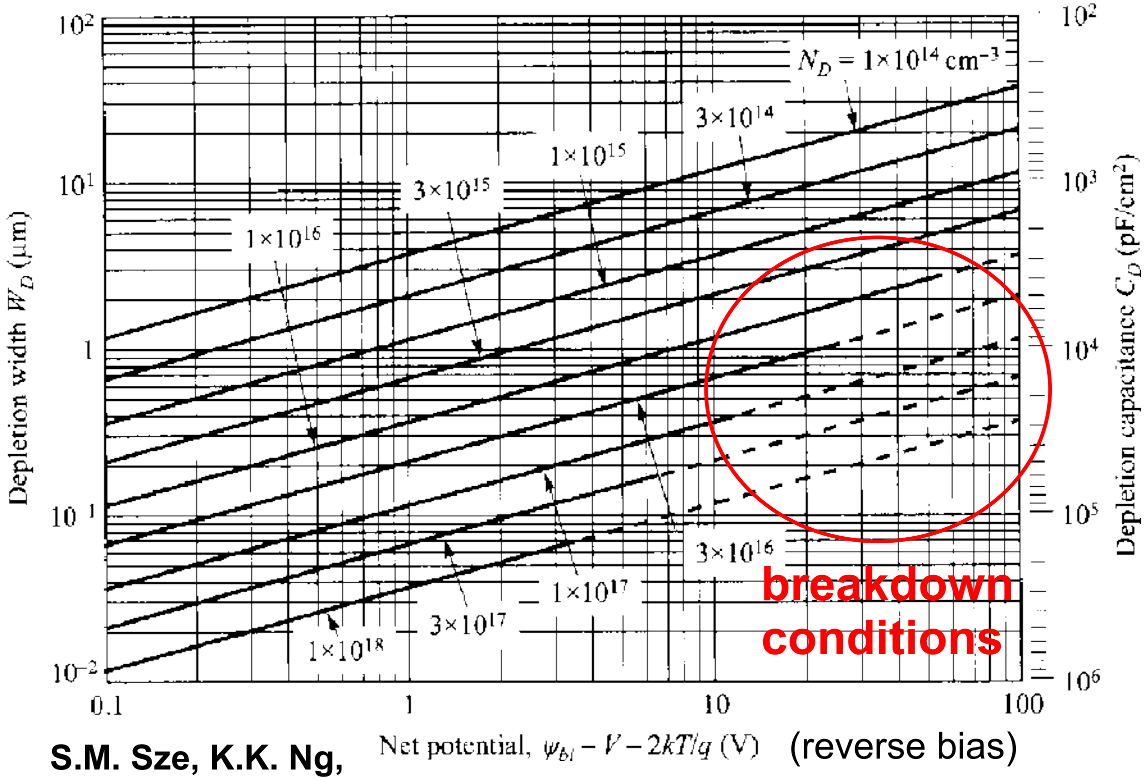

S.M. Sze, K.K. Ng, Wiley, 2007

$$W_D = W_{Dp} + W_{Dn} = \sqrt{\frac{2\epsilon_s}{q}\left(\frac{N_A + N_D}{N_A N_D}\right)(\Psi_{bi} - V)}$$

width of the depletion zone

- APD ~ one-sided abrupt junction (p^+-n or n^+-p)

$$W_D = \sqrt{\frac{2\epsilon_s}{qN}(\Psi_{bi} - V)}$$

(with $N=N_D$ for $N_A>>N_D$ and vice versa)

- depletion zone capacitance

$$C_D = \frac{\epsilon_s}{W_D} = \sqrt{\frac{q\epsilon_s N}{2}(\Psi_{bi} - V)} \quad F/cm^{-2}$$

I-V Characteristic

- p-n junction under bias voltage
  - forward bias ($pn>n_i^2$)
  - reverse bias ($pn<n_i^2$)
- total current through ideal diode

$$J = J_p + J_n = J_0\left[\exp\left(\frac{qV}{kT}\right) - 1\right]$$

- with saturation current

$$J_0 = \frac{qD_p n_i^2}{L_p N_D} + \frac{qD_n n_i^2}{L_n N_A} = J_0(T)$$

- 60mV of voltage increase raise forward current by one decade
- important deviation: junction breakdown

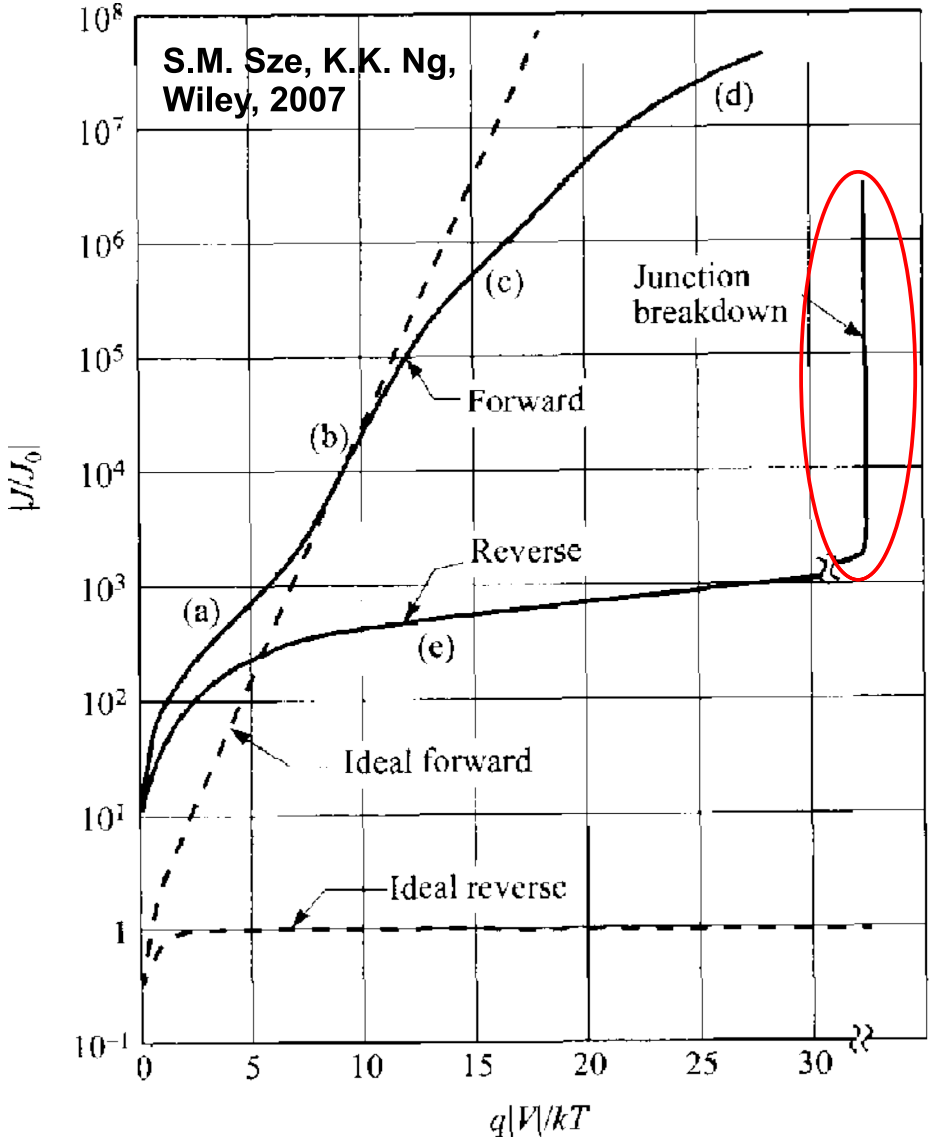

Junction Breakdown I

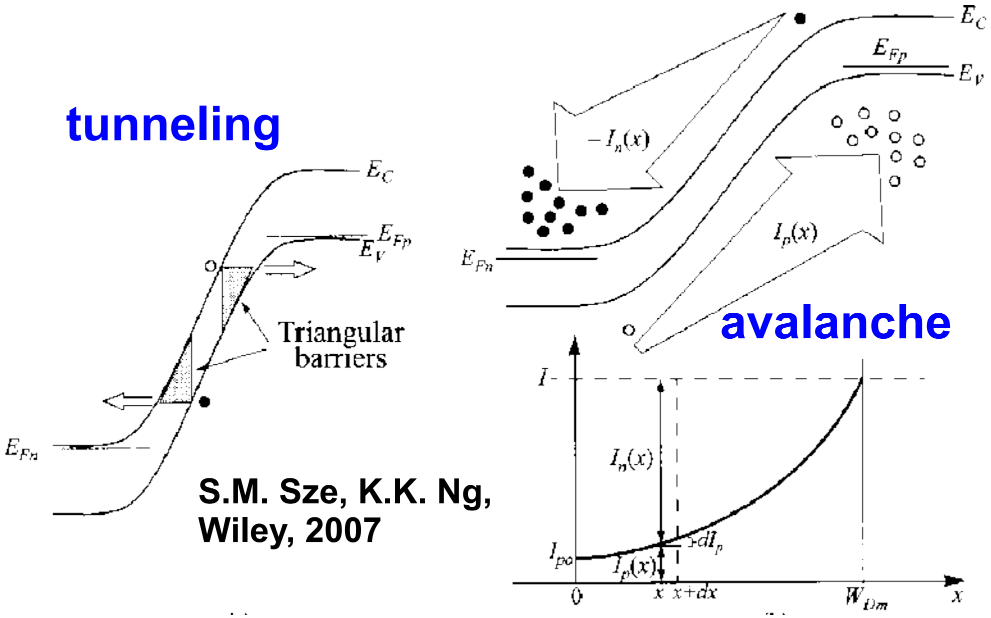

S.M. Sze, K.K. Ng, Wiley, 2007

$$\int_0^{W_{Dm}} \alpha_p \exp\left[-\int_0^x (\alpha_p - \alpha_n)\, dx'\right] dx = 1$$

condition for hole-initiated breakdown

$$\int_0^{W_{Dm}} \alpha_n \exp\left[-\int_x^{W_{Dm}} (\alpha_n - \alpha_p)\, dx'\right] dx = 1$$

condition for electron-initiated breakdown

- breakdown mechanisms
  - thermal instability
  - tunneling breakdown
  - avalanche breakdown
- example: break down initiated by hole current I_{p0}

$$dI_p = I_p \alpha_p\, dx + I_n \alpha_n\, dx$$

- hole multiplication factor

$$M_p \equiv \frac{I}{I_{p0}}$$

- $M_p \sim \infty$ at breakdown

$$1 - \frac{1}{M_p} = \int_0^{W_{Dm}} \alpha_p \exp\left[-\int_0^x (\alpha_p - \alpha_n)\, dx'\right] dx$$

Junction Breakdown II

- breakdown voltage

$$V_{BD} = \frac{E_m W_{Dm}}{2} = \frac{\epsilon_s E_m^2}{2qN} \quad V$$

- (approximation) for various semiconductors

$$V_{BD} \approx 60 \left(\frac{E_g}{1.1 eV} \right)^{3/2} \left(\frac{N}{10^{16} cm^{-3}} \right)^{-3/4} \quad V$$

S.M. Sze, K.K. Ng, Wiley, 2007

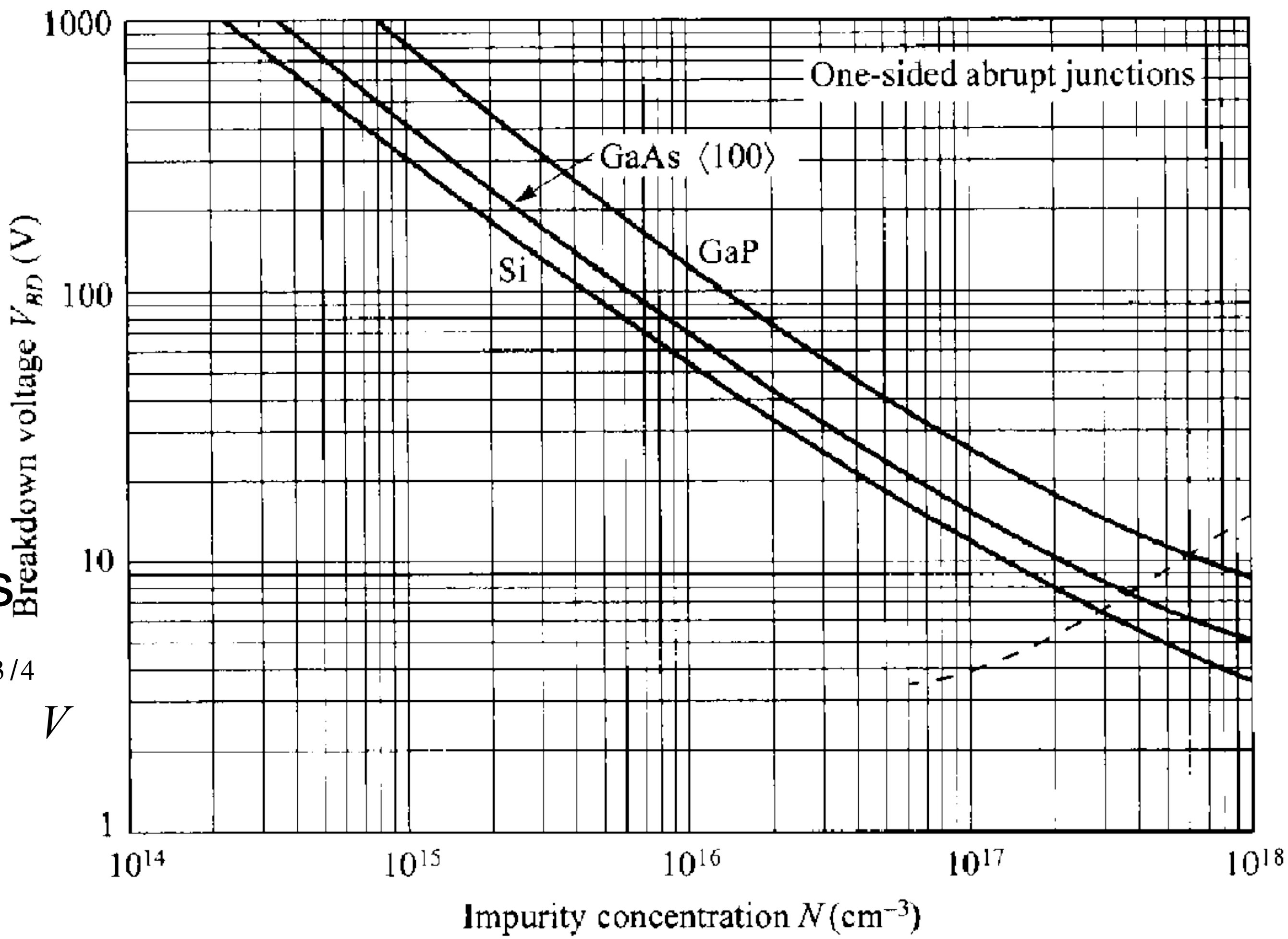

Junction Breakdown III

- depletion layer width has strong *N* dependence

- electric field at breakdown only varies very slowly with *N*

S.M. Sze, K.K. Ng, Wiley, 2007

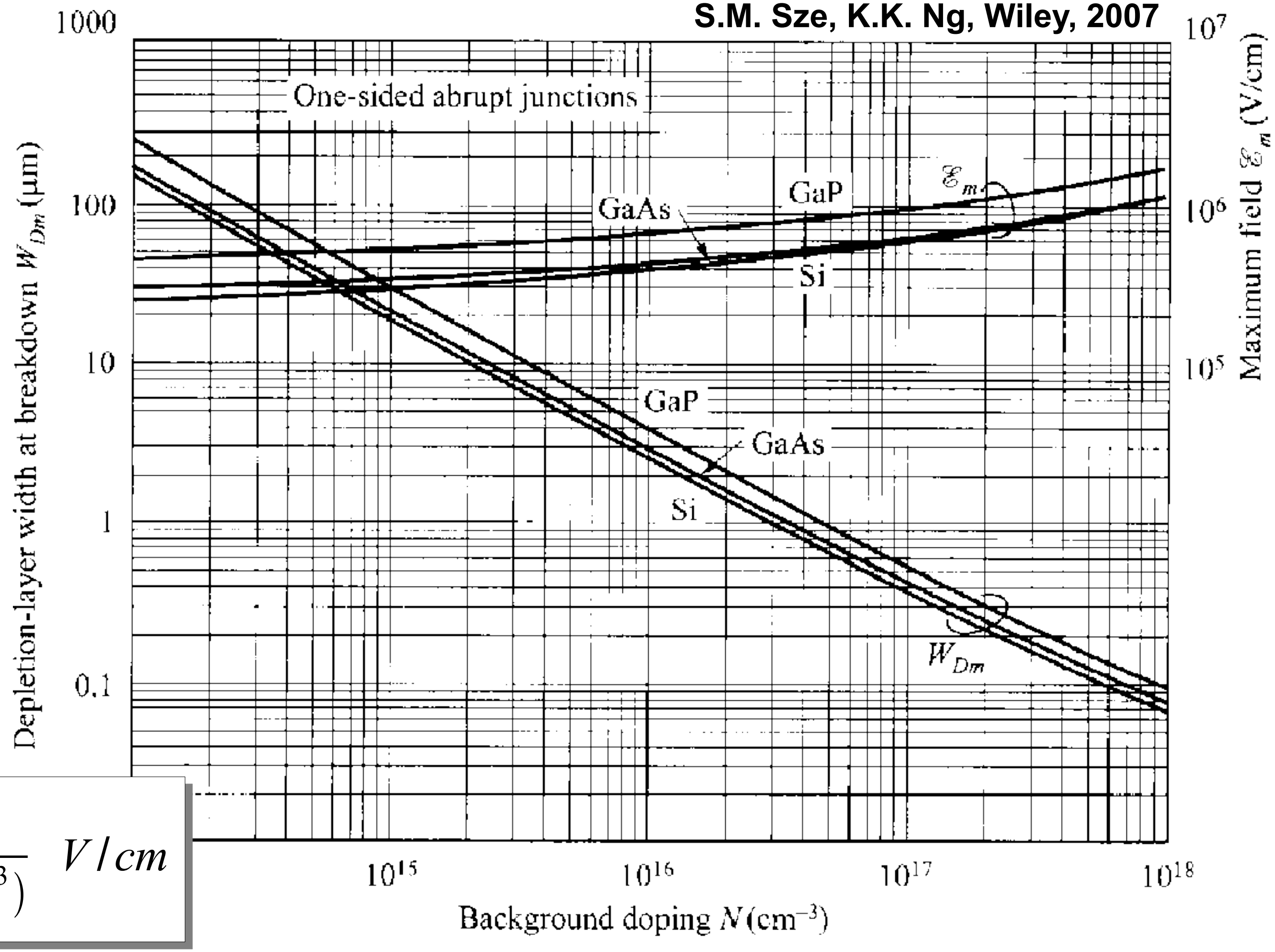

$$E_m = \frac{4\times 10^5}{1-(1/3)\log_{10}(N/10^{16}\,cm^{-3})}\ V/cm$$

RWTH AACHEN UNIVERSITY

Summary of Part II

- ideal: abrupt p-n junctions ('simple' calculations, field properties)
- maximum electric field at the interface between the n- and p-doped areas
- width of depletion zone depends on doping and bias voltage and typically is about 0.1 – 10 μm
- depletion zone acts as capacitance which is inversely proportional to the width of the zone
- p-n junction shows a breakdown at large reverse bias which can be used for the amplification of the initiating charge carriers

III. Photodetectors

Optical Properties of Silicon

$$\lambda = \frac{hc}{\Delta E} = \frac{1240}{\Delta E(eV)}\ nm$$

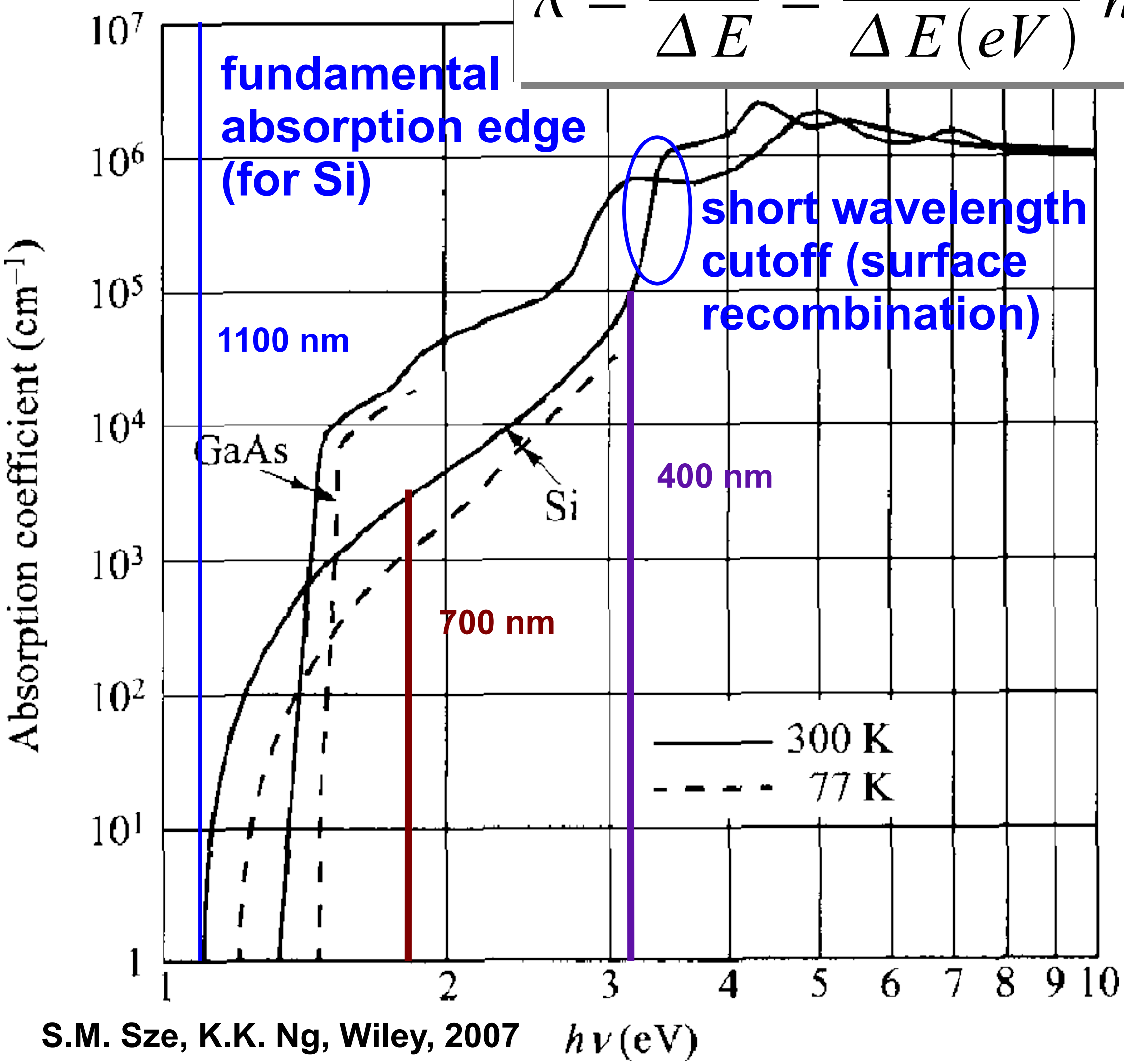

S.M. Sze, K.K. Ng, Wiley, 2007

- coefficient α determines strength (and depth) of absorption
  - small λ: absorption near surface
  - large λ: light can penetrate deeper into semiconductor

→ determines quantum efficiency

- thin devices (α*W_D 'not large')
  - multiple reflections → consider reflection and transmission

Photodetectors

- classification (gain & structure)
  - photoconductor
    gain : variable
  - photodiode (p-n, p-i-n, ...)
    gain : ≤ 1
  - avalanche photodiode (APD)
    gain : 10^2 - 10^4
  - Geiger-mode APD
    gain : 10^5 - 10^6

- basic working principle
  - carrier generation by incident light
  - carrier transport in electric field
  - photo current → output signal

- quantum efficiency

$$\eta = \frac{I_{phot}}{q\,\Phi_{phot}} = \frac{N_{pe}}{N_\gamma}, \quad \eta = \eta(\lambda)$$

- photosensitivity / responsivity

$$S = \frac{I_{phot}}{P_{opt}} = \frac{I_{phot}}{\Phi_{phot}\,h\nu} = \eta\,\frac{\lambda(nm)}{1240} \quad A/W$$

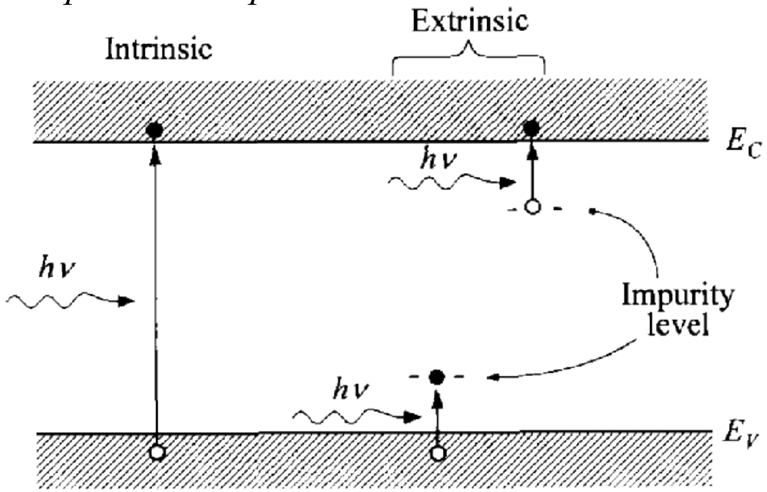

S.M. Sze, K.K. Ng, Wiley, 2007

Photodiode I

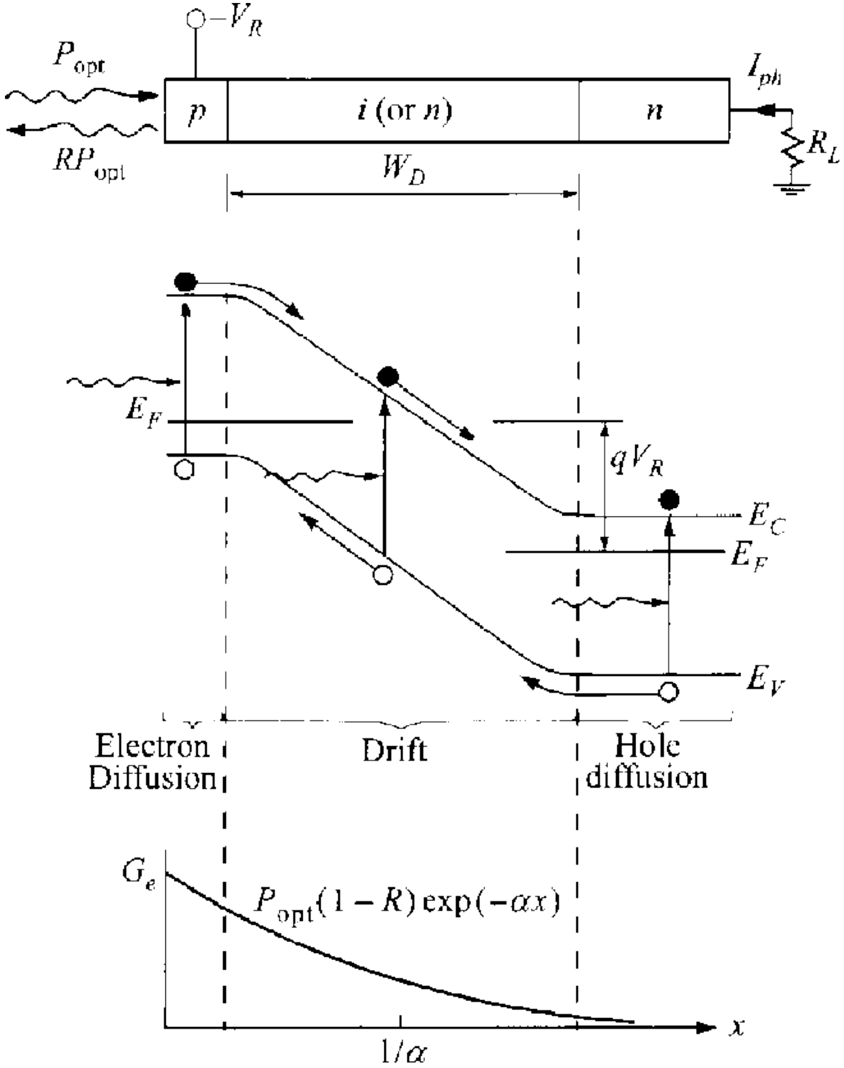

S.M. Sze, K.K. Ng, Wiley, 2007

- p-n junction or p-i-n type (intrinsic layer can be adjusted to optimize quantum efficiency)
- separation of electron-hole pairs generated by high electric field
- electron-hole generation rate

$$G_e(x) = \Phi_0 \alpha\, exp(-\alpha x)$$

- drift current

$$J_{dr} = -q \int_0^{W_D} G_e(x)\,dx = q\,\Phi_0\left[1-\exp(-\alpha W_D)\right]$$

- quantum efficiency

$$\eta = (1-R)\left[1-\frac{\exp(-\alpha W_D)}{1+\alpha L_p}\right]$$

Photodiode II

- internal quantum efficiency can be optimized by adjusting the width of the depletion zone to the wave length
- narrow widths are desirable for telecommunications (transit time of carriers introduces phase shift between photon flux and photocurrent)

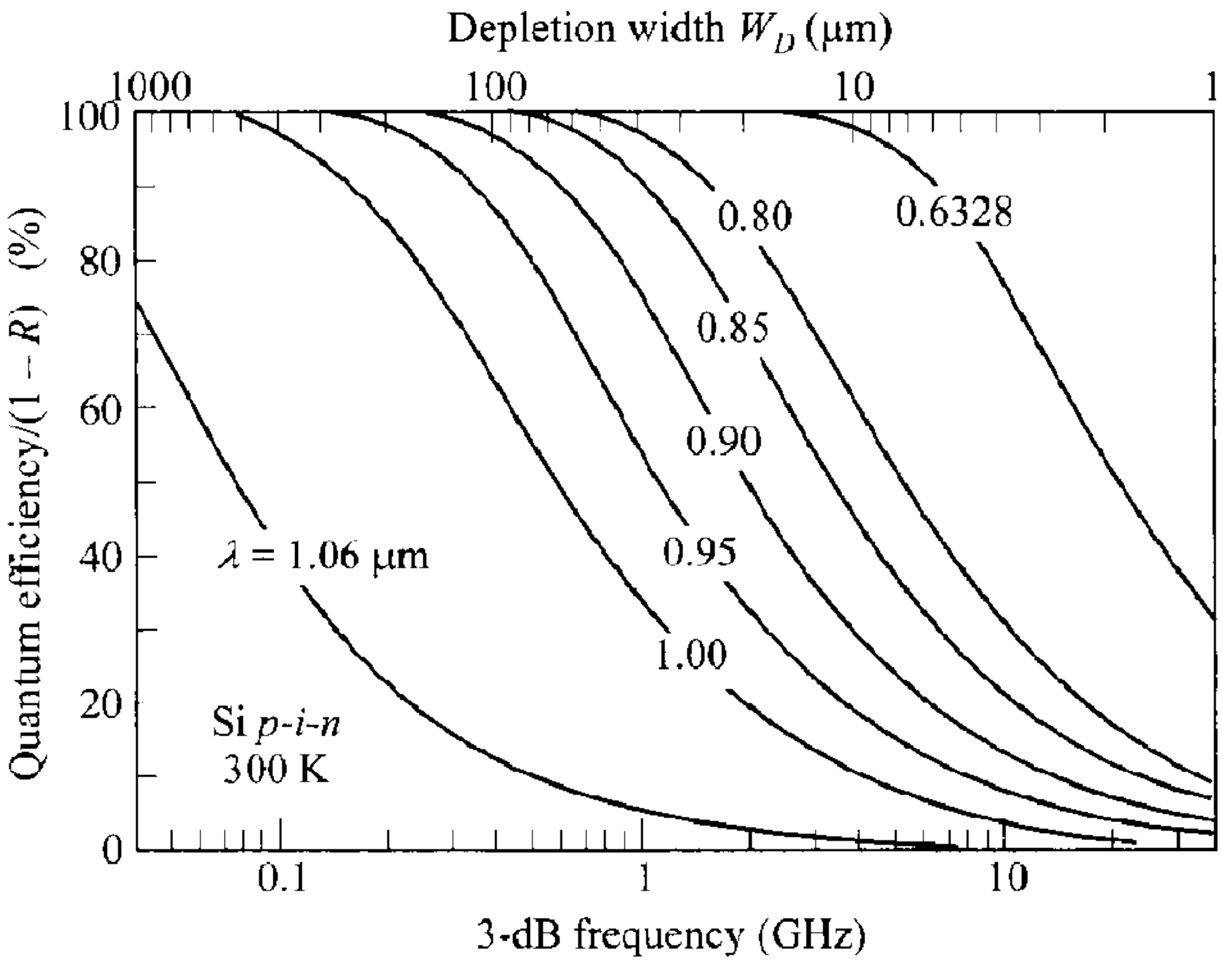

S.M. Sze, K.K. Ng, Wiley, 2007

Avalanche Photodiode I

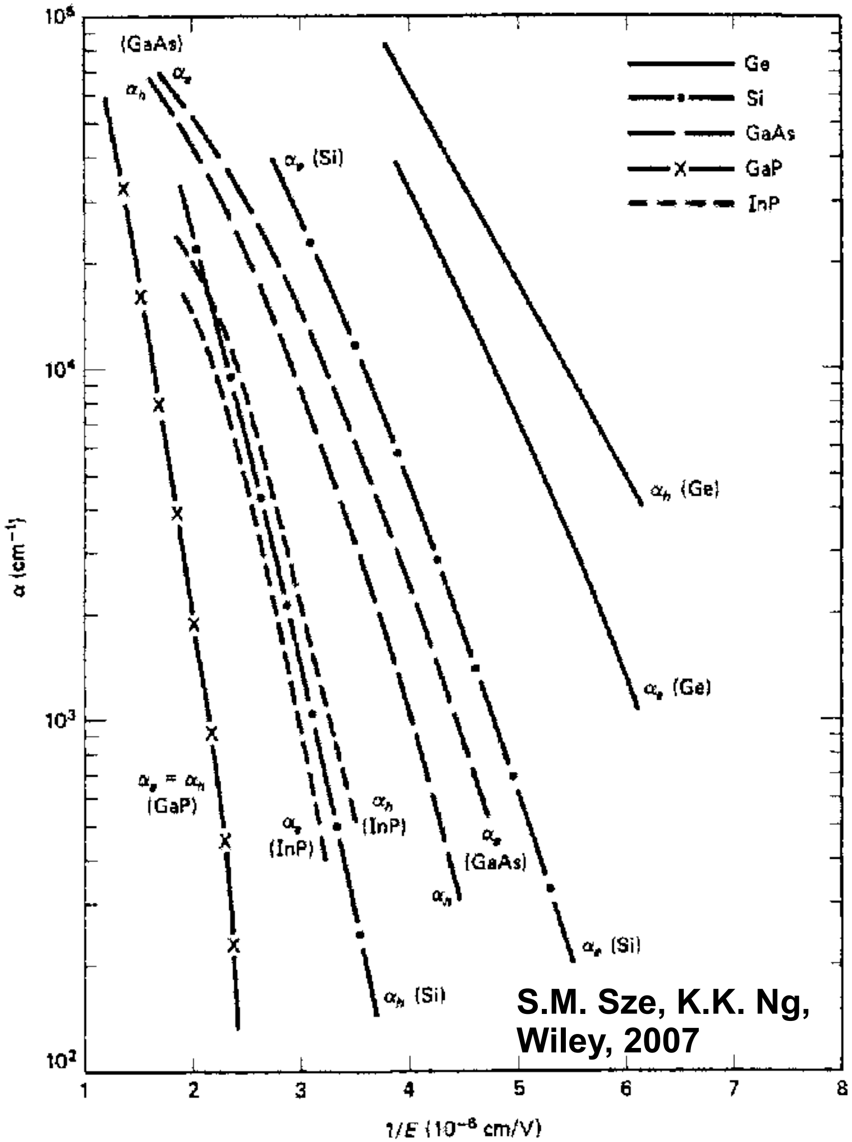

- operated at high reverse bias
  → electron ionization is dominant
- electron multiplication factor

$$M = \left\{ 1 - \int_0^{W_D} \alpha_n \exp\left[- \int_x^{W_D} (\alpha_n - \alpha_p)\, dx' \right] dx \right\}^{-1}$$

- practical limit of photomultiplication

$$M_{ph,\,max} = \sqrt{\frac{V_B}{n I_p R_s}}$$

V_B: breakdown voltage

I_p : primary photocurrent

R_s: effective series resistance

n: constant depending on semiconductor

Avalanche Photodiode II

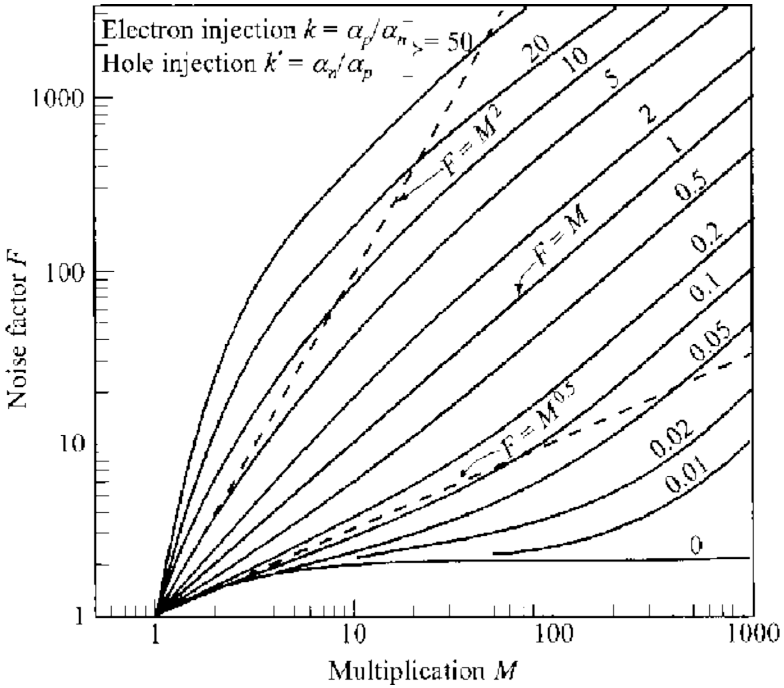

S.M. Sze, K.K. Ng, Wiley, 2007

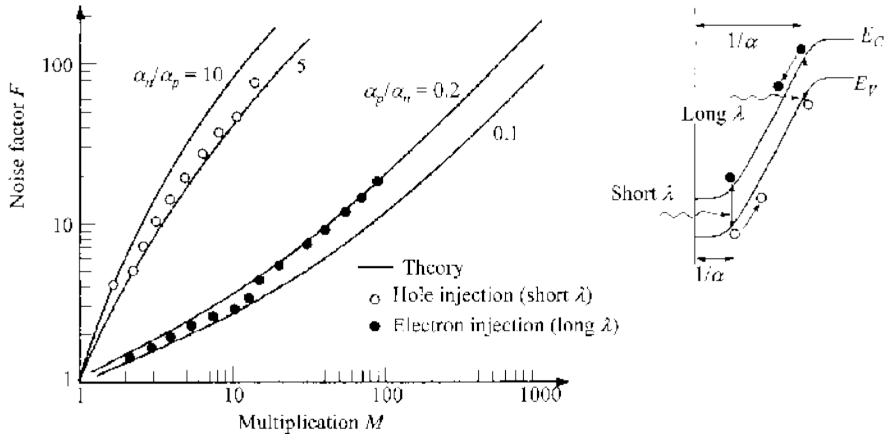

- electron-hole creation is statistical process → excess noise factor

$$F(M) = \frac{\langle M^2 \rangle}{\langle M \rangle^2} = \frac{\langle M^2 \rangle}{M^2}$$

- describes increase of shot noise w.r.t. noiseless APD
- for electron injection ($k=\alpha_p/\alpha_n$)

$$F(M) \approx kM + \left(2 - \frac{1}{M}\right)(1-k)$$

($k=0 \rightarrow F(M)=2$, $k=1 \rightarrow F(M)=M$)

- high multiplication noise is bad for single photon counting...

Avalanche Photodiode III

- optimum wavelength range for silicon APDs: 600 – 800 nm
  - 100% QE can be reached
- hole-to-electron ionization coeff. ratio *k* depends on E field
  - 0.1 (at 3×10^5 V/cm) to 0.5 (6×10^5 V/cm)

  → control noise by
  - keeping E field as low as possible
  - initiate avalanche by electrons
- APD profiles
  - large drift region (sat. velocity)
  - small avalanche region
  - use p-on-n (short wavelengths) or n-on-p (long wavelengths) types

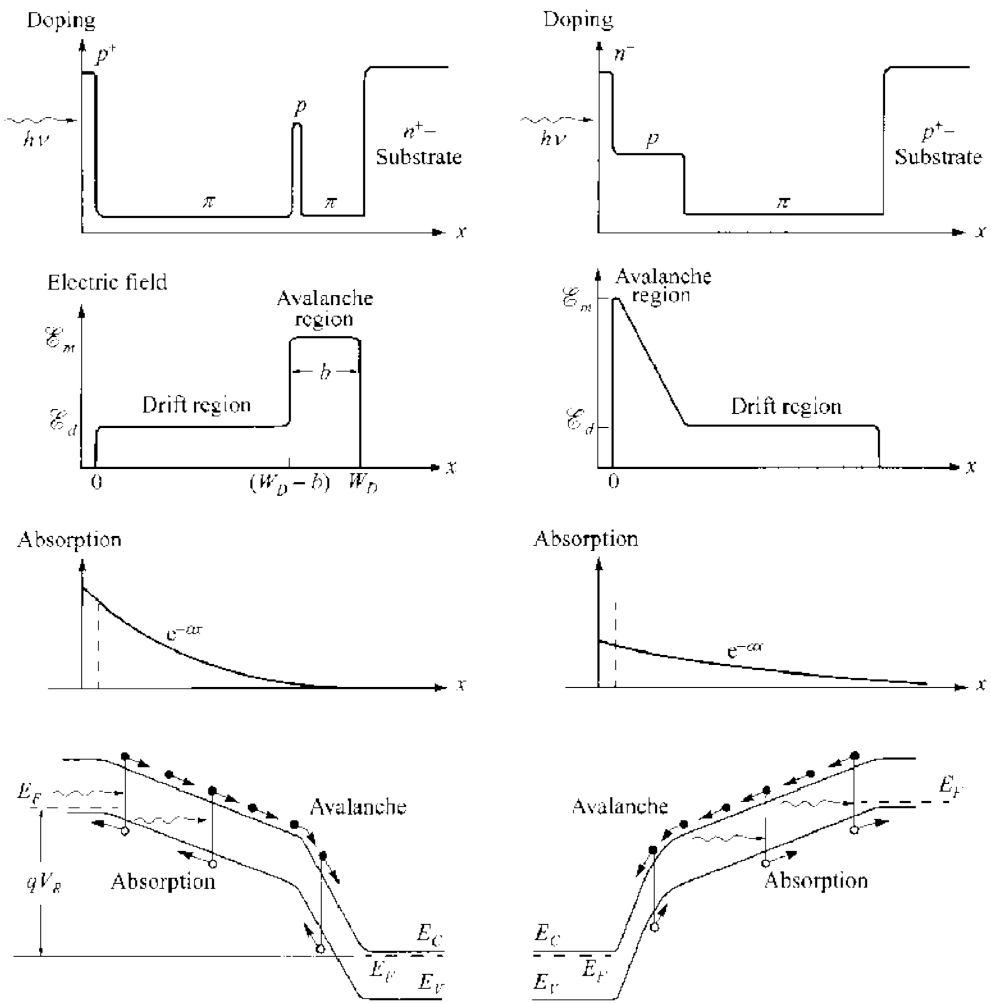

S.M. Sze, K.K. Ng, Wiley, 2007

Geiger-mode APD

- in a GAPD the field is so high that electrons AND holes contribute to avalanche breakdown

- positive feedback, requires external 'quenching' mechanism

- quenching: reduce electric field by reducing V_{op}
  - passive queching: resistor
  - active quenching

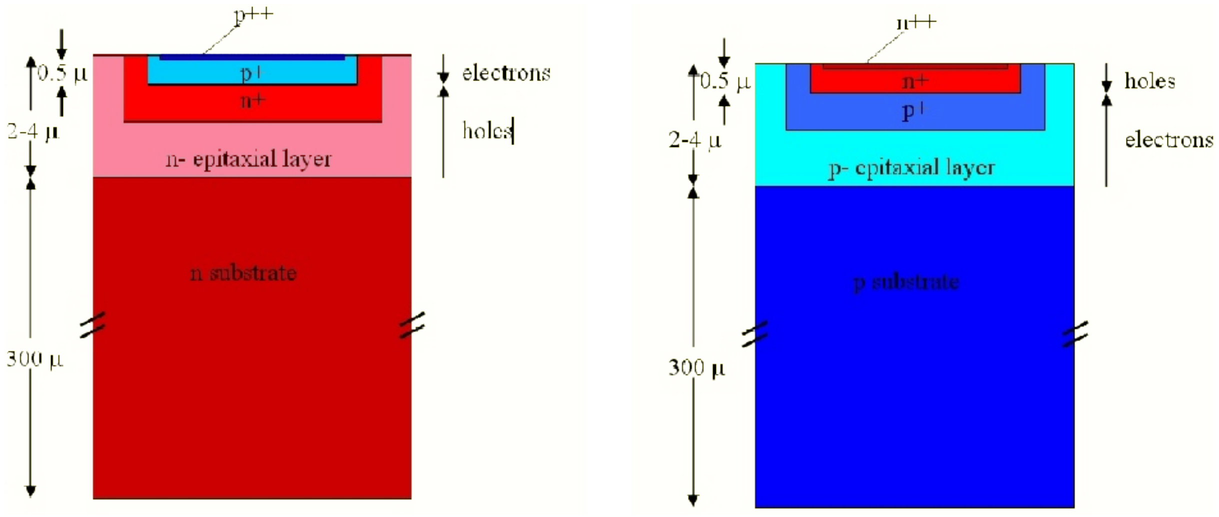

D. Renker, E. Lorenz, J.Inst.4 (2009), p04004

→ SiPM: combination of a number of small GAPD cells

Summary of Part III

- absorption properties of silicon are ideal for optical photons
- electron-hole pairs are generated in the depletion zone of a p-n junction and separated by an electric field
- internal quantum efficiency is determined by the width of the depletion zone and the absorption properties for the respective wave lengths; antireflective coatings optimize the total quantum efficiency
- avalanche photodiodes work at large reverse bias voltages (several tens of volts) and multiply the initially produced carriers
- structure of APD (p-on-n, n-on-p) determines the sensitivity w.r.t. the wave length and the noise properties
- GAPDs work at even higher voltages → higher multiplication, but the avalanche breakdown has to be quenched externally

IV. Silicon Photomultipliers

Silicon Photomultipliers

- arrays of GAPDs are nowadays called SiPM, MPPC, SSPM, …
- SiPMs have positive and negative aspects w.r.t. photomultiplier tubes:

+

- SiPM pros
  - high photo detection efficiency
  - photon-number resolving
  - low operating voltage
  - insensitive to large B fields
  - 'low' price
  - 'standard chip technology'

−

- SiPM cons
  - dark count rate
  - afterpulsing
  - optical cross talk
  - sensitive area

SiPM Operation I

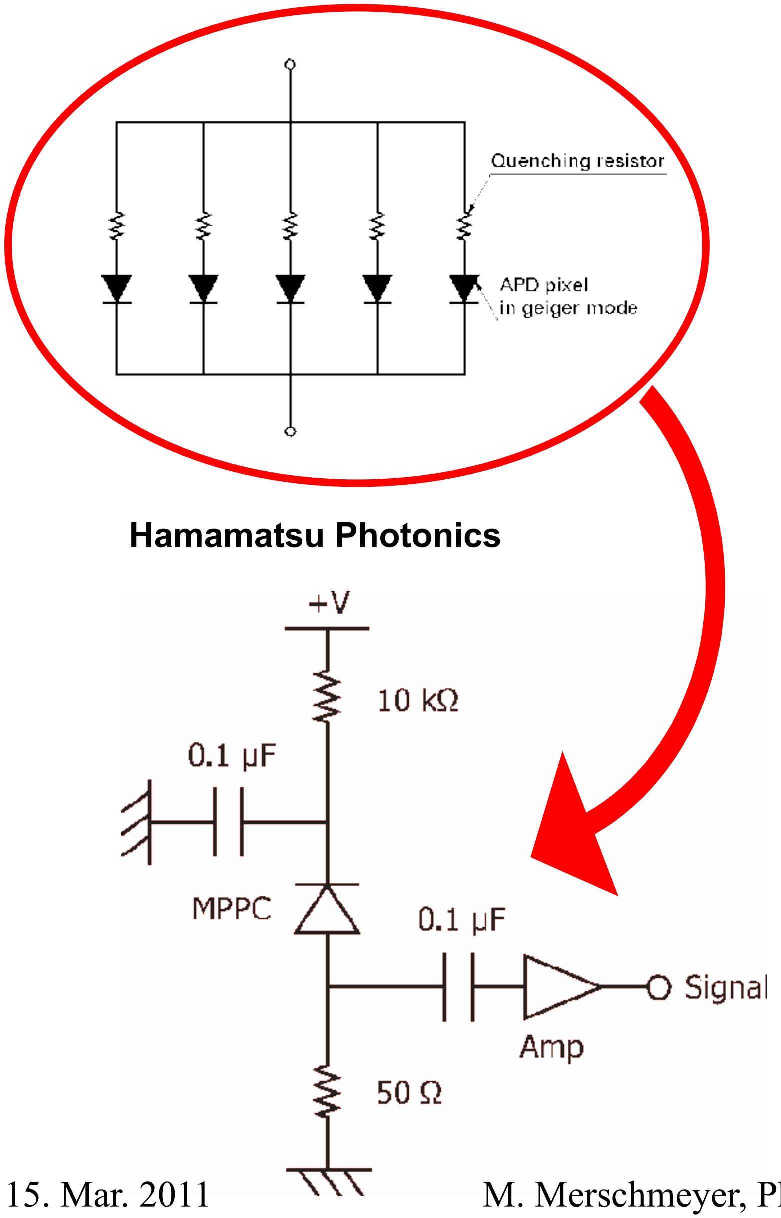

- operated at reverse bias $V_{op} > V_{bd}$ (→ overvoltage)

$$V_{ov} = V_{op} - V_{bd}$$

- sum of multiple APD output pulses results in large pulse
- charge from single APD cell

$$Q_{cell} = C_{cell} \times \left(V_{op} - V_{bd}\right)$$

- linear gain

$$G_{lin} = Q_{cell} \times N_{pe}$$

- a photon can fire more than one cell (opt. crosstalk, afterpulsing) → real gain (~ 10^5 to 10^6)

$$G_{real}\left(V_{ov}\right) \geqslant G_{lin}$$

SiPM Operation II

J. Rennefeld, RWTH Aachen

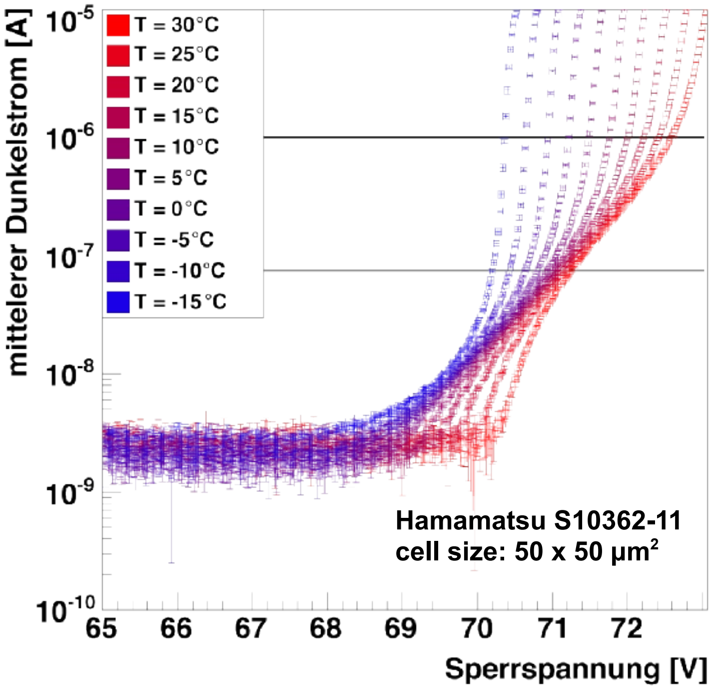

Hamamatsu Photonics

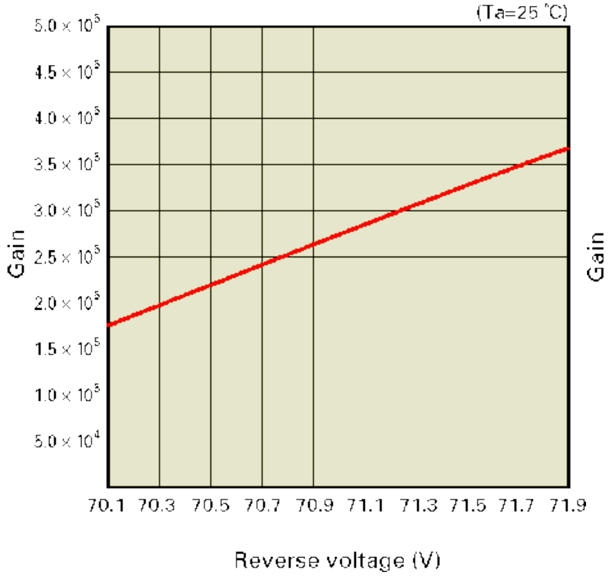

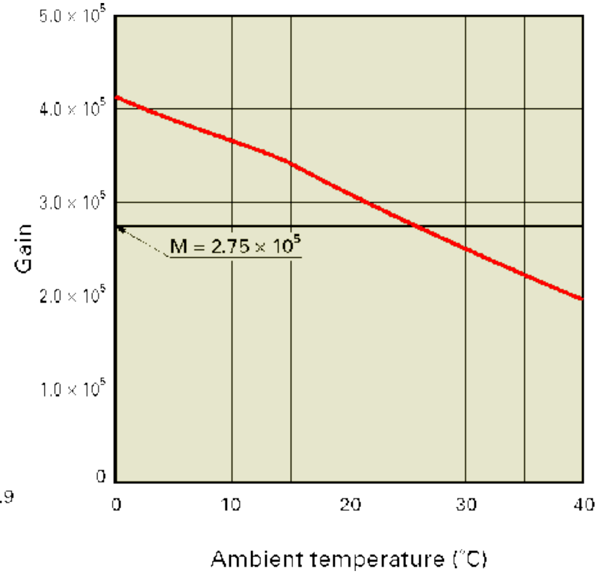

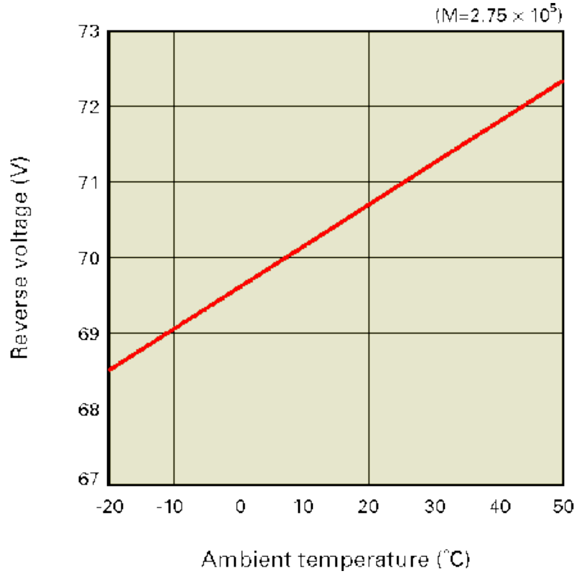

- SiPM is very sensitive to operating conditions
  - breakdown voltage V_{bd} (and other parameters) depend on ambient temperature T
  - overvoltage V_{ov} needs adjustment

SiPM Operation III

J. Schumacher, M Lauscher, RWTH Aachen

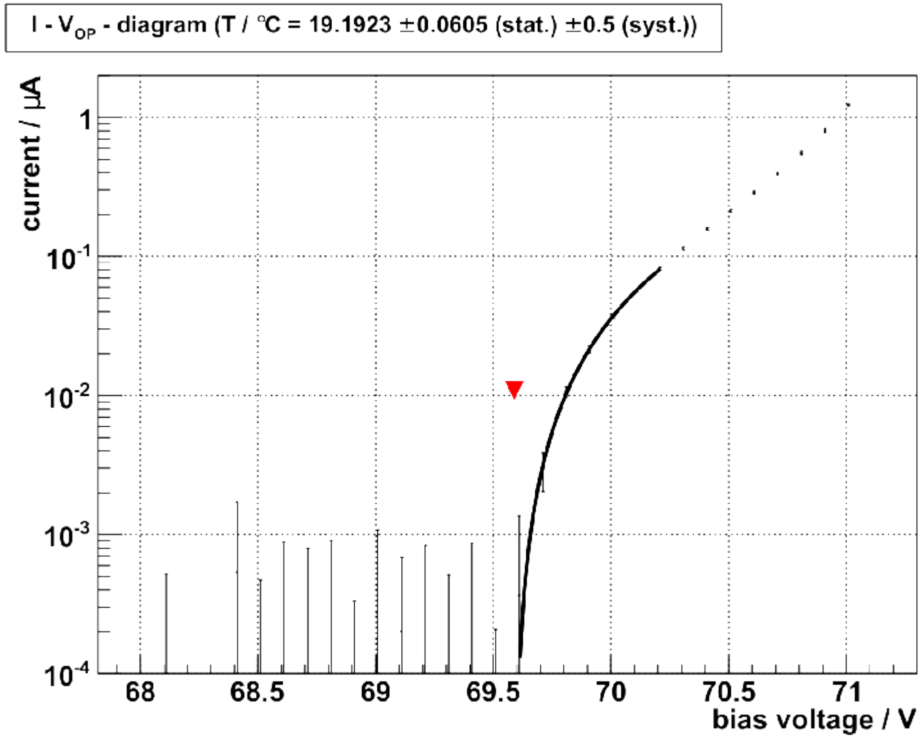

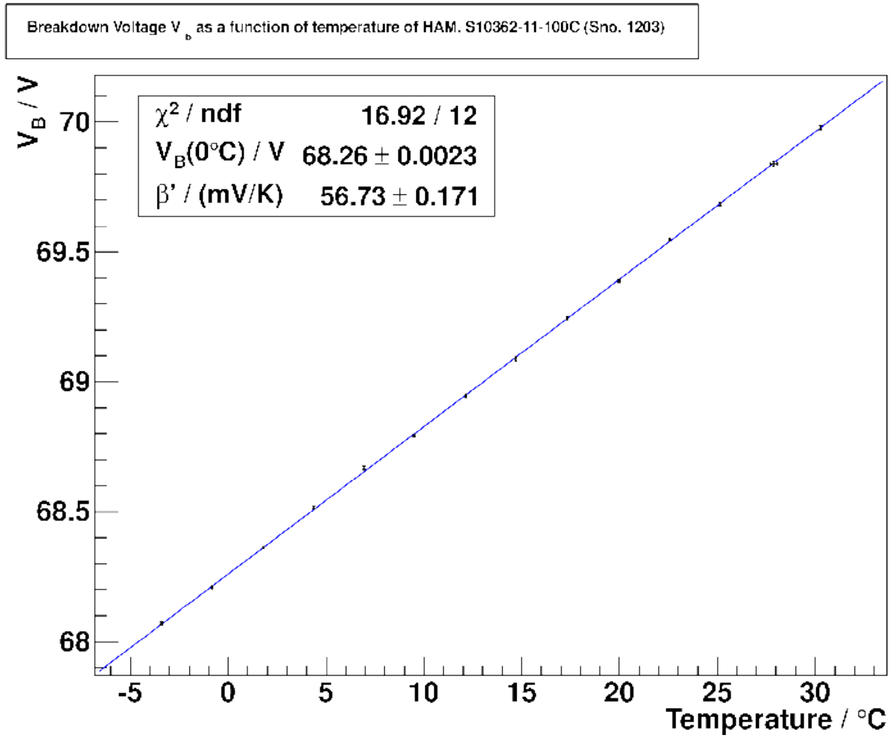

- at breakdown voltage → substantial change of dark current
- temperature coefficient of 56mV/K confirmed

SiPM I-V Characteristic

- SiPM is basically a diode and a series resistor → typical I-V characteristics
- quenching resistors limit the forward current

$$R_{tot} \sim \left(\sum_{N_{cell}} R_{quench}^{-1} \right)^{-1}$$

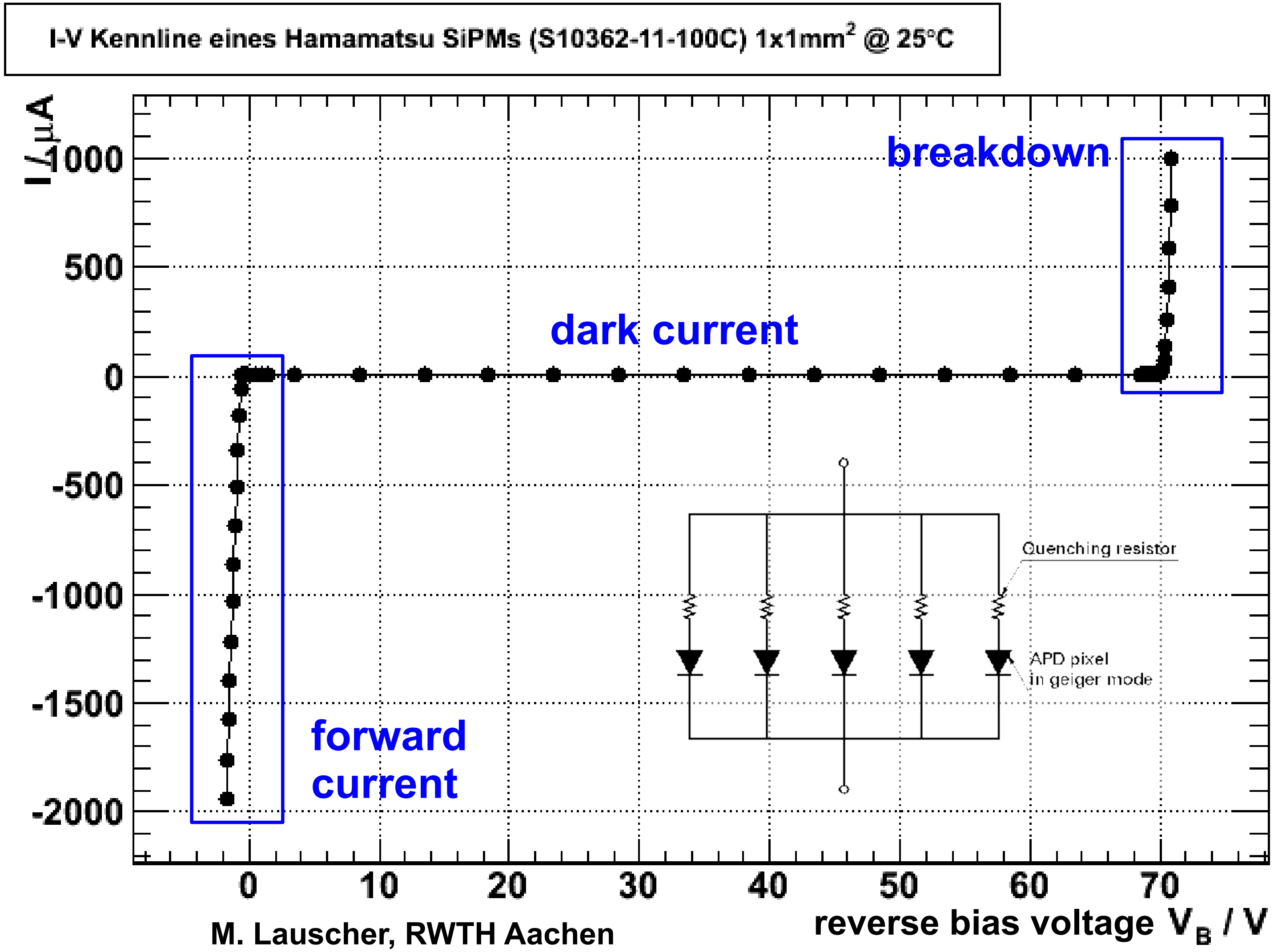

SiPM I-V Characteristic: Zoom

- forward bias region shows expected behavior (diode+series resistor)
- reverse bias region has 'initeresting' features

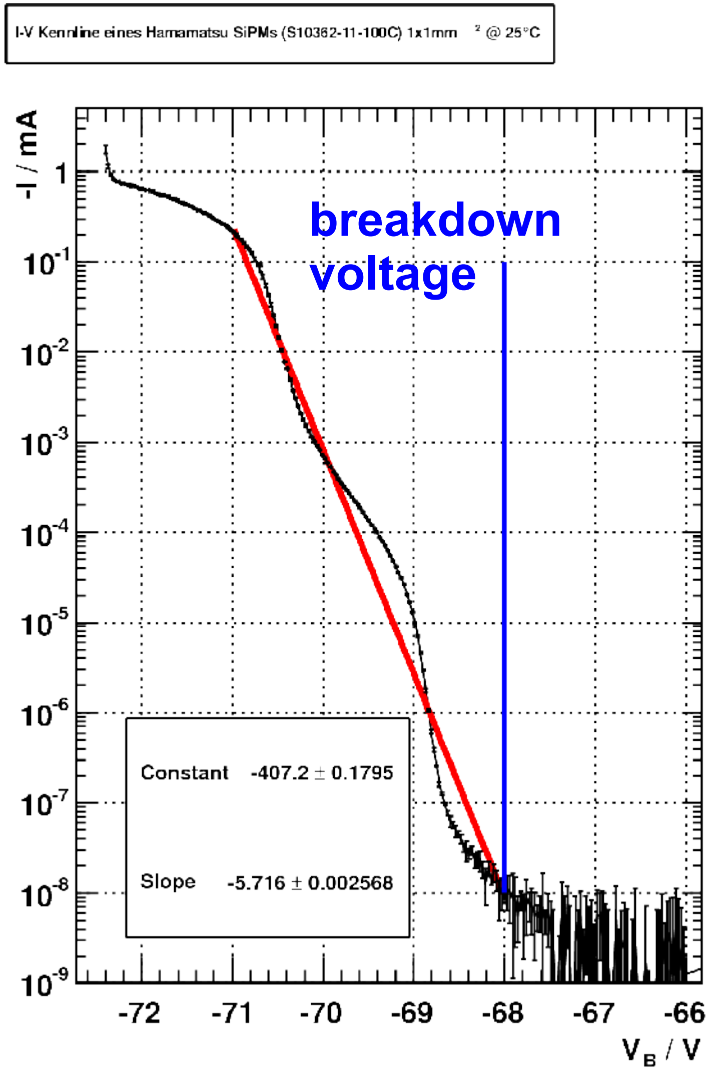

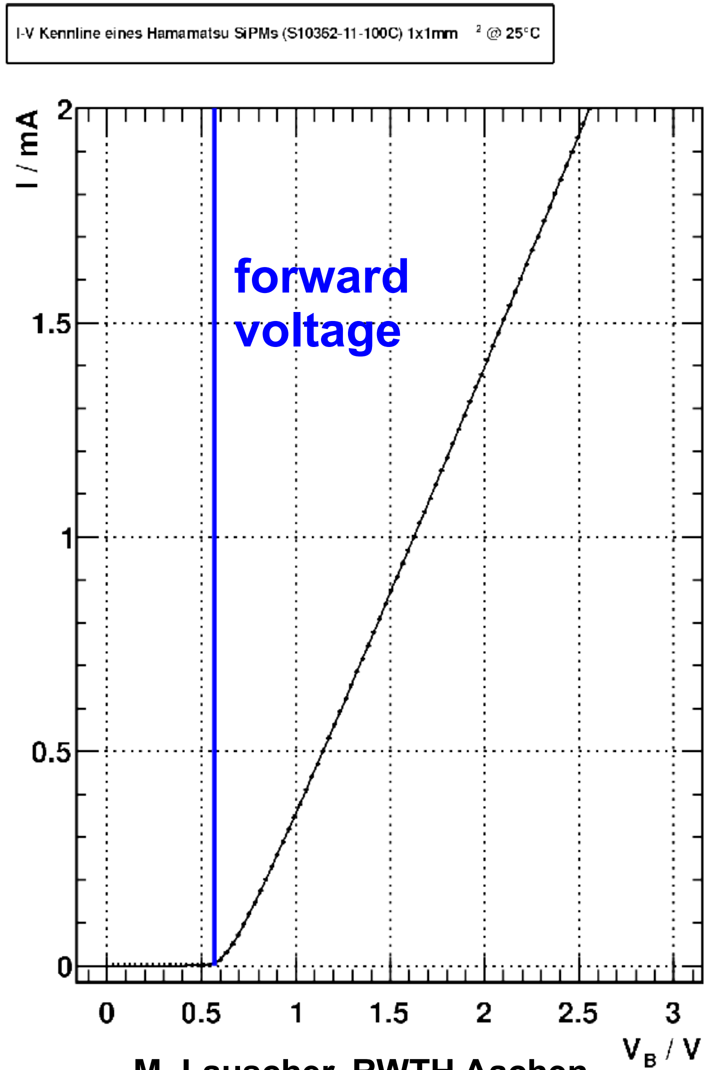

SiPM I-V Characteristic: Resistivity

- SiPM exhibits approximate ohmic behavior at large reverse bias as well as for a sufficient forward voltage
  - R_{tot} ~ [redacted]
  - N_{cell} = 100

→ R_{quench} ~ [redacted]

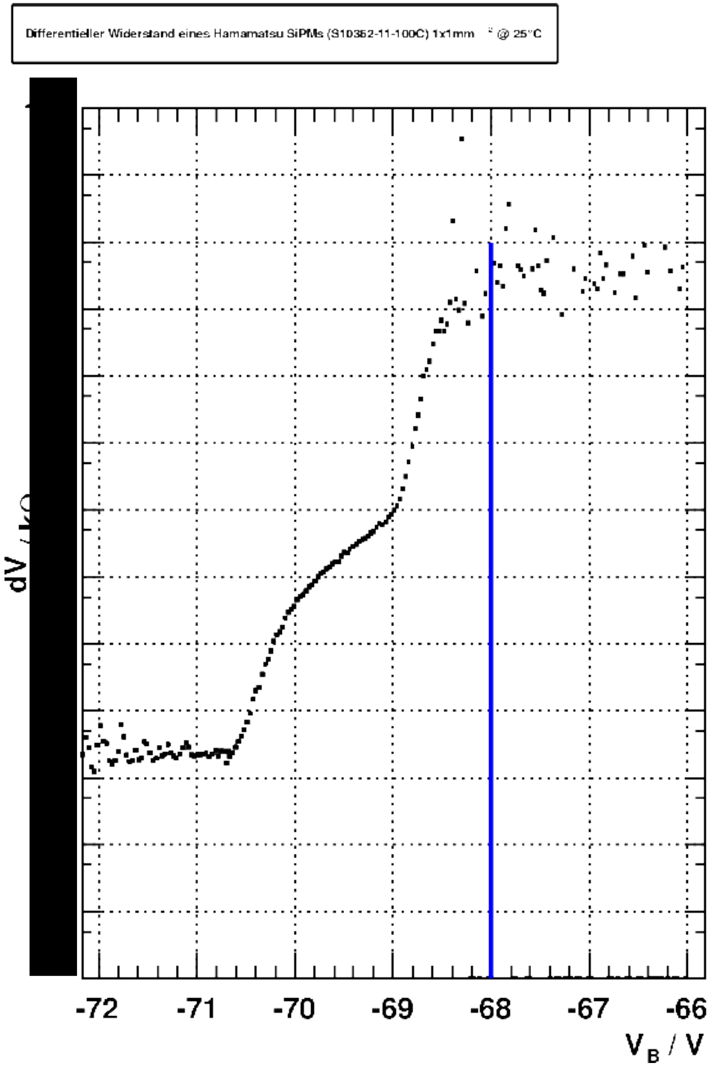

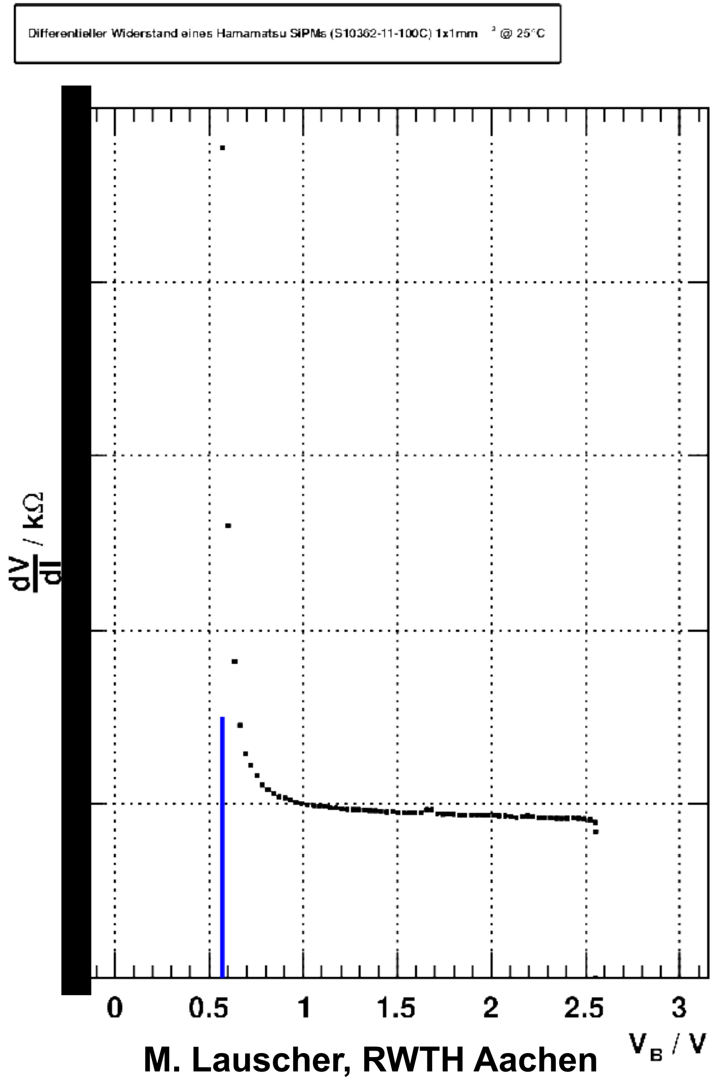

SiPM Output

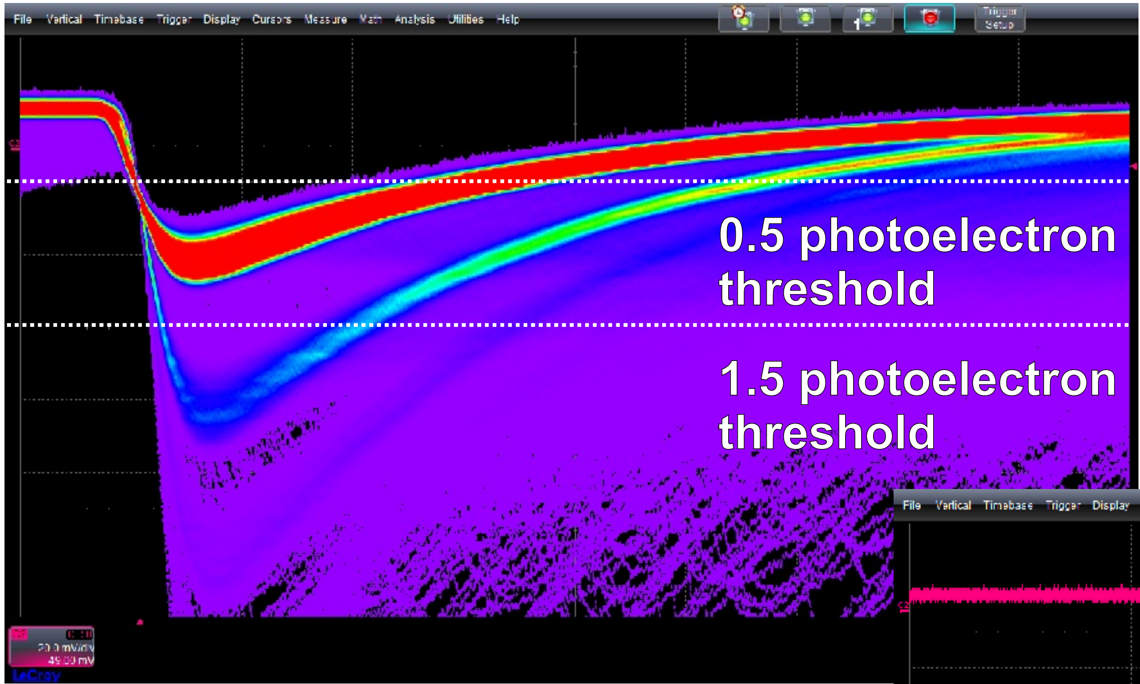

- intensity spectrum of the SiPM signal shows discrete and equidistant peaks
- cleanliness depends on SiPM type, V_{op}, T and the background light flux

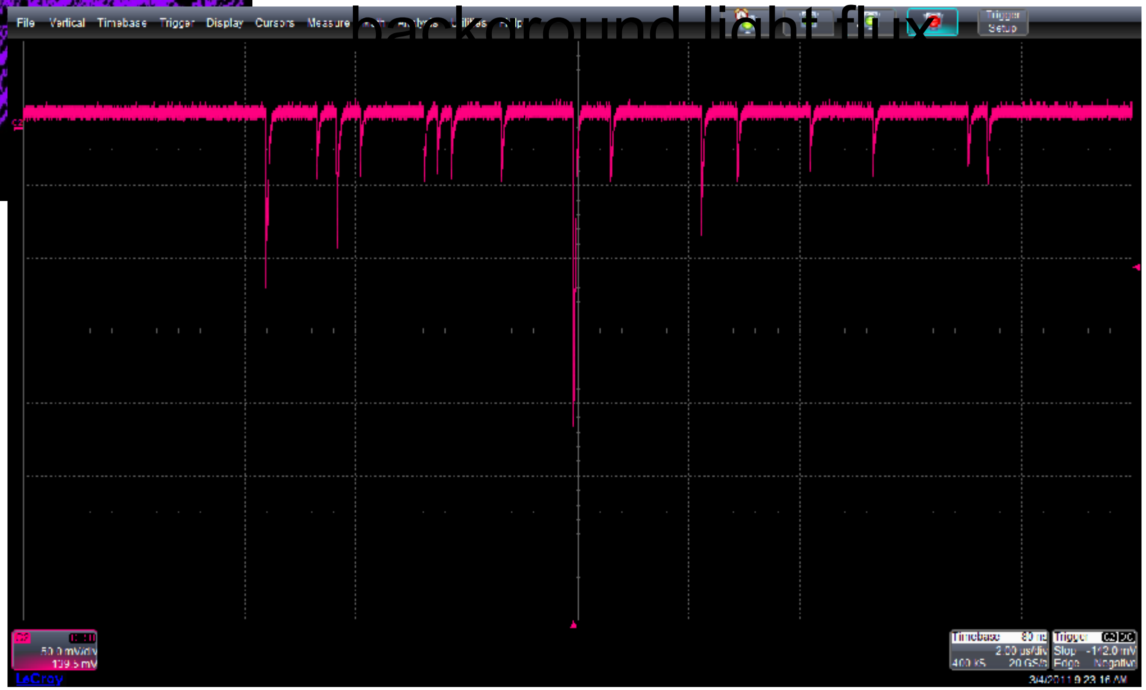

- discrete peak heights → discrete charge spectrum
- resolution depends on charge integration time window

SiPM Output

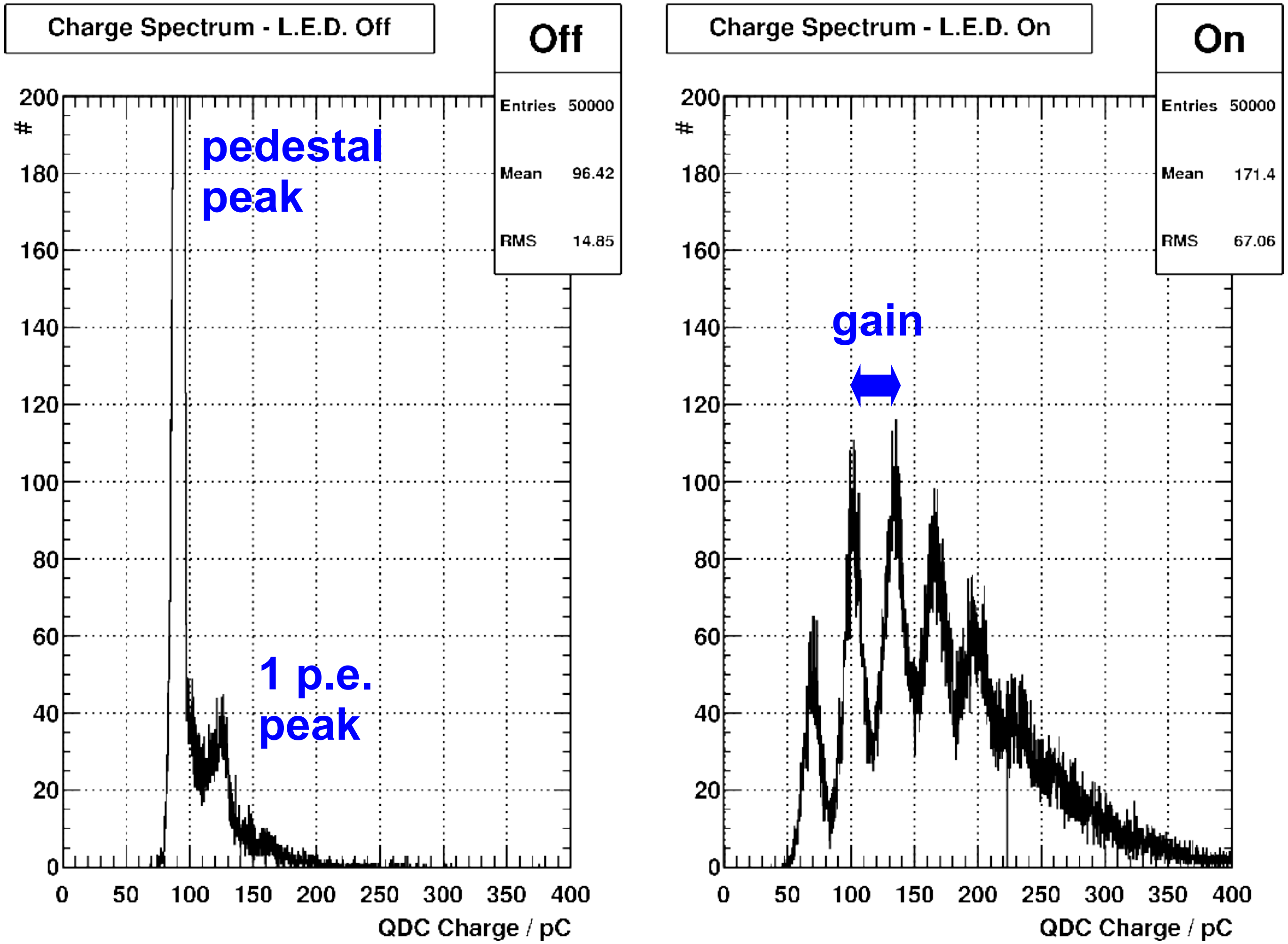

M. Lauscher, RWTH Aachen

- charge integration yields 'finger spectra'
  - pedestal peak
  - photoelectron peaks
- good pixel uniformity: SiPM → quasi-analog photon detector
- gain (incl. amplifier) can be extracted
- get average number of photoelectrons from pedestal:

$$p(k) = e^{-\langle N_{pe}\rangle} \cdot \frac{\langle N_{pe}\rangle^k}{k\,!}$$

$$\langle N_{pe}\rangle = -\ln\left(p(0)\right)$$

Dark Count Rate

- SiPMs are noisy: typical DCR at 0.5 p.e. threshold is 0.1 – 1 MHz (per mm²)
- thermal generation of carriers and contributions from afterpulses and optical cross talk
- two-cell noise for SiPM with single cell noise R_1 ~ 1 kHz, time window $\tau \leq$ 100 ns

$$R_2 = 2\tau R_1^2 = 0.2\,s^{-1}$$

$$R_{2,tot} \sim \binom{N_{cell}}{2} \cdot R_2 \approx N_{cell}^2 \cdot 0.1\,s^{-1}$$

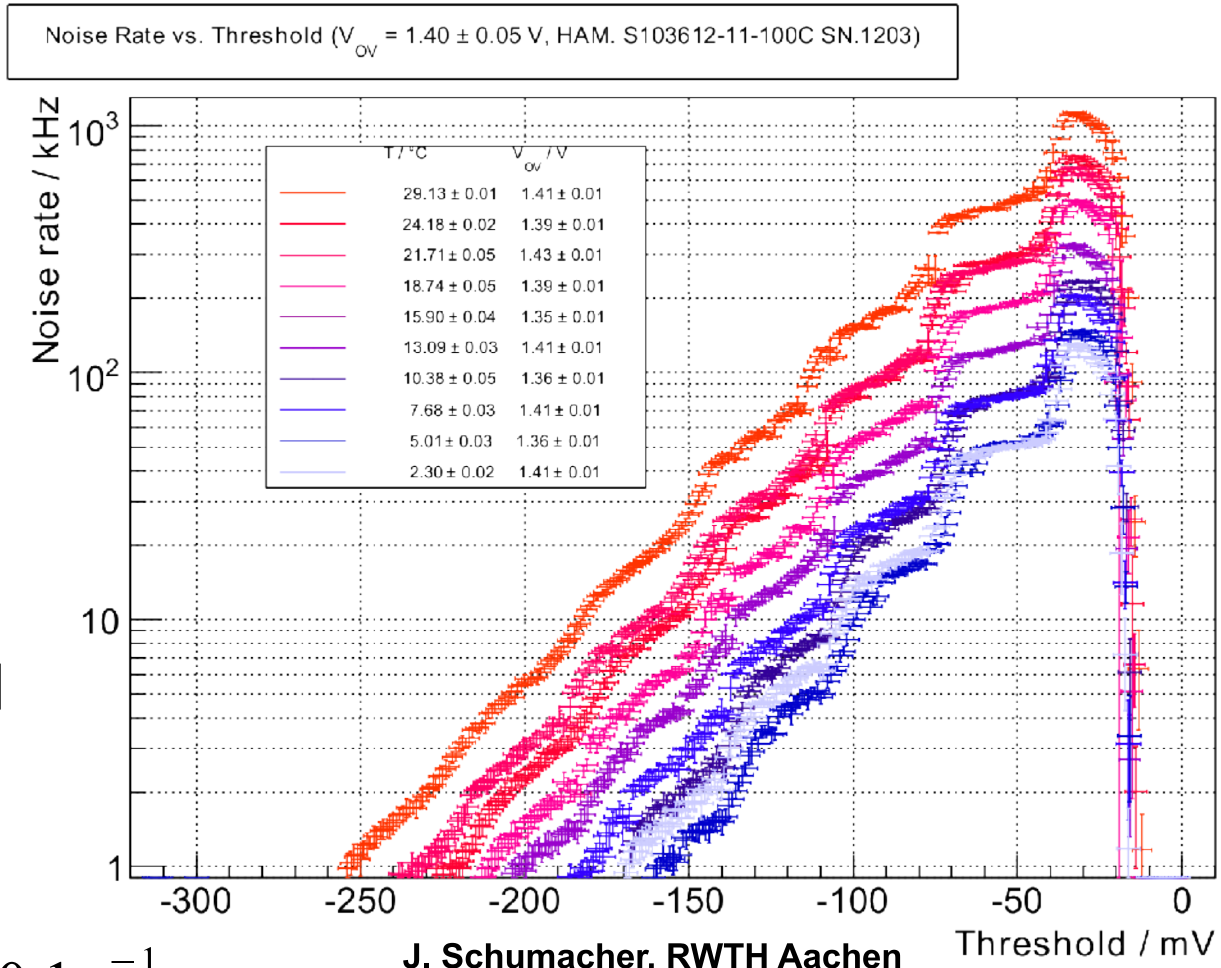

J. Schumacher, RWTH Aachen

Photo Detection Efficiency (PDE)

$$PDE(\lambda, V_{op}, T) = QE(\lambda, T) \times FF \times P_{av}(V_{op}, T)$$

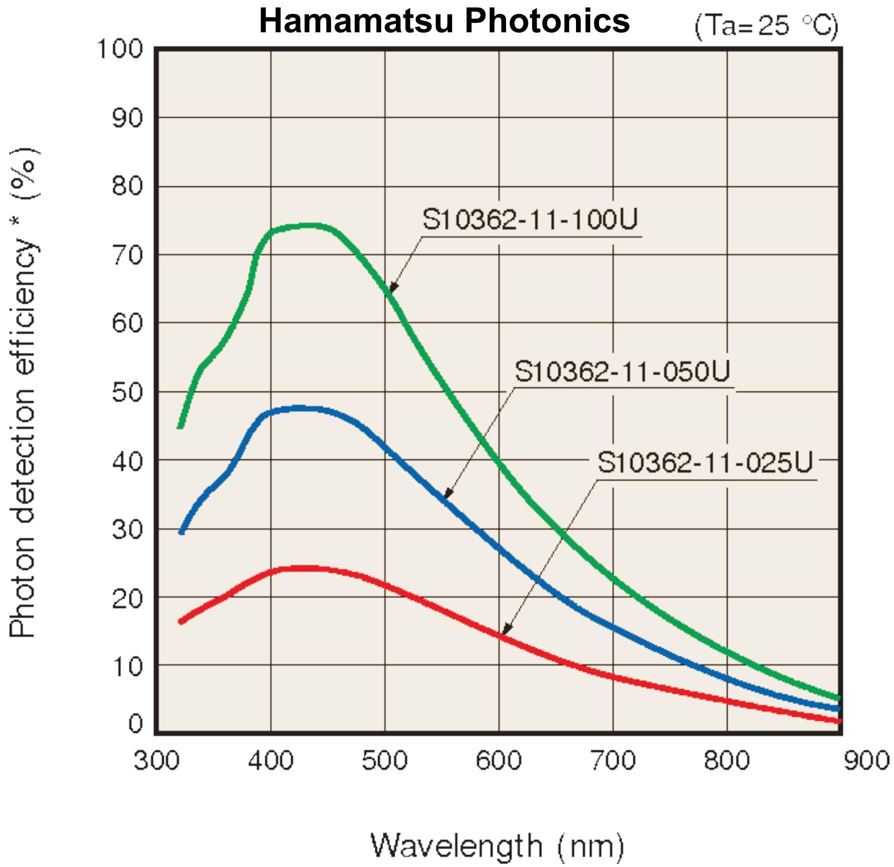

* Photon detection efficiency includes effects of crosstalk and afterpulses.

- PDE = probability to detect a single photon at a threshold of about 0.5 p.e.
- depends on
  - quantum efficiency (*QE*)
  - cell geometry (fill factor *FF*)
  - avalanche trigger probability (P_{av})
- determination:
  - average amount of incoming photons in given time interval (fixed λ): $\langle N_\gamma \rangle$
  - get $\langle N_{pe} \rangle$ from pedestal fraction

$$PDE(\lambda) = \langle N_{pe} \rangle / \langle N_\gamma \rangle$$

Quantum Efficiency

- absorption of optical photons in silicon has strong wavelength dependence

$$I(x) \sim \exp(-\alpha x)$$

- dimensions of depletion zones ~ O(1 μm)
  - $\alpha = 10^4\ \mathrm{cm}^{-1} \rightarrow$ 63% of light absorbed within 1 μm (99.995% within 10 μm)
  - $\alpha = 10^6\ \mathrm{cm}^{-1} \rightarrow$ 63% of light absorbed within 0.01 μm (~100% within 1 μm)
- device optimization must consider
  - wave length of incoming light
  - width of depletion zone
  - antireflective coatings at the surface

S.M. Sze, K.K. Ng, Wiley, 2007

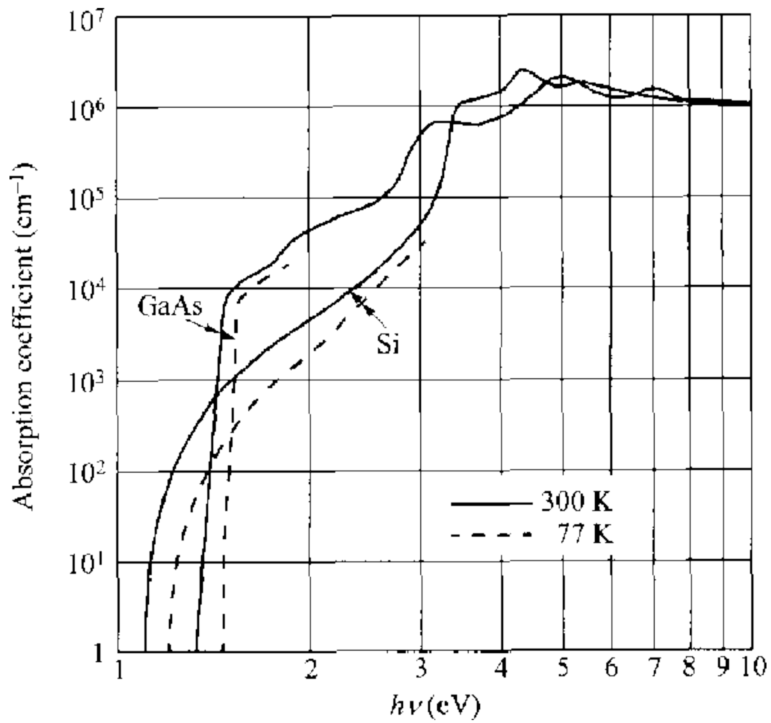

SiPM Geometry: Fill Factor

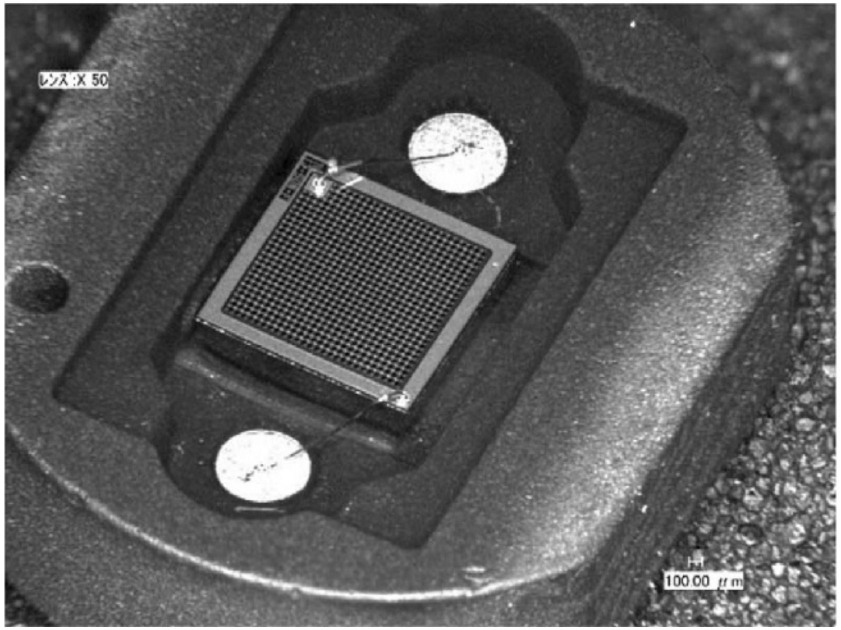

M. Yokoyama et al.,
NIM A610 (2009) 362

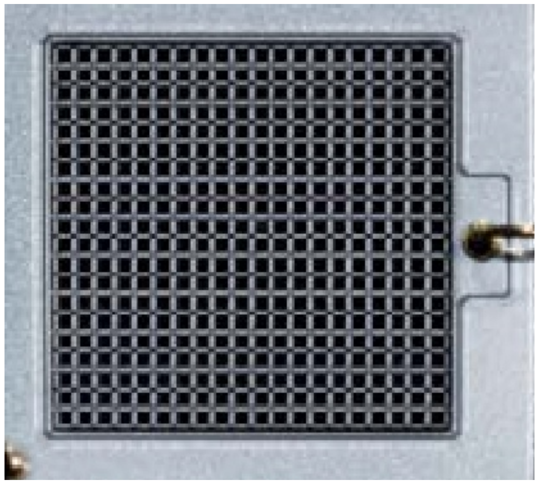

Hamamatsu
Photonics

- cell separation and quenching resistor cause insensitive space between cells

  → geometrical fill factor

$$FF = \frac{active\ \ area}{total\ \ cell\ \ area}$$

- depends on cell size (e.g. for Hamamatsu S10362 series)
  - about 80% for 100 x 100 μm^2
  - about 30% for 25 x 25 μm^2
- solutions
  - integrate quenching resistor into silicon bulk material

Avalanche Probability

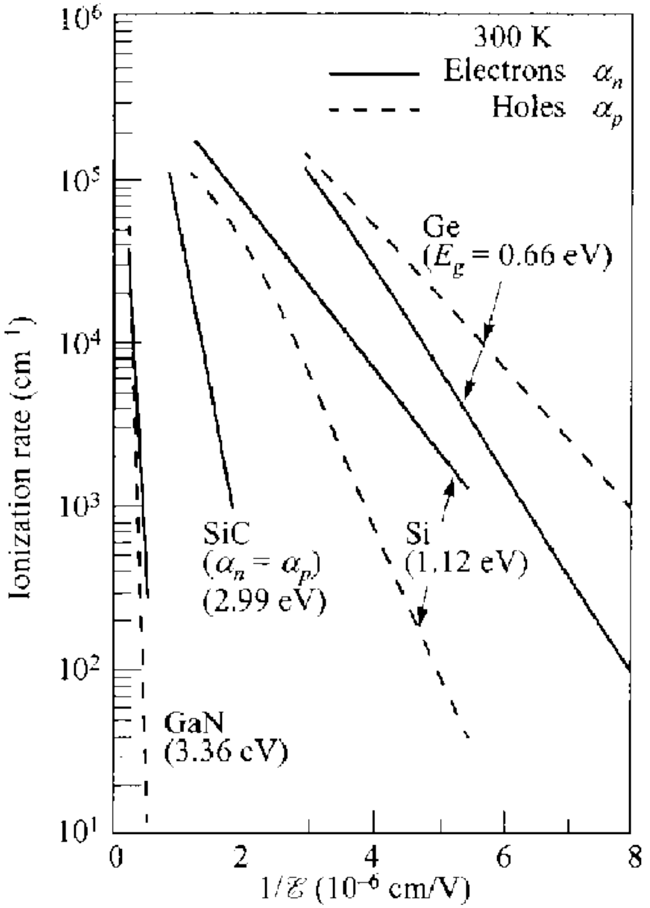

S.M. Sze, K.K. Ng, Wiley, 2007

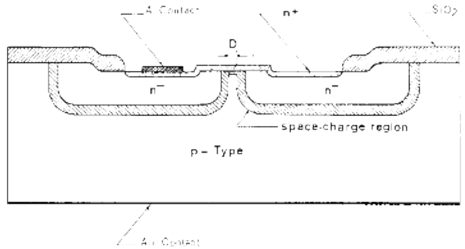

W. Oldham et al., IEEE Tr. El. Dev. 19 (1972) 1056

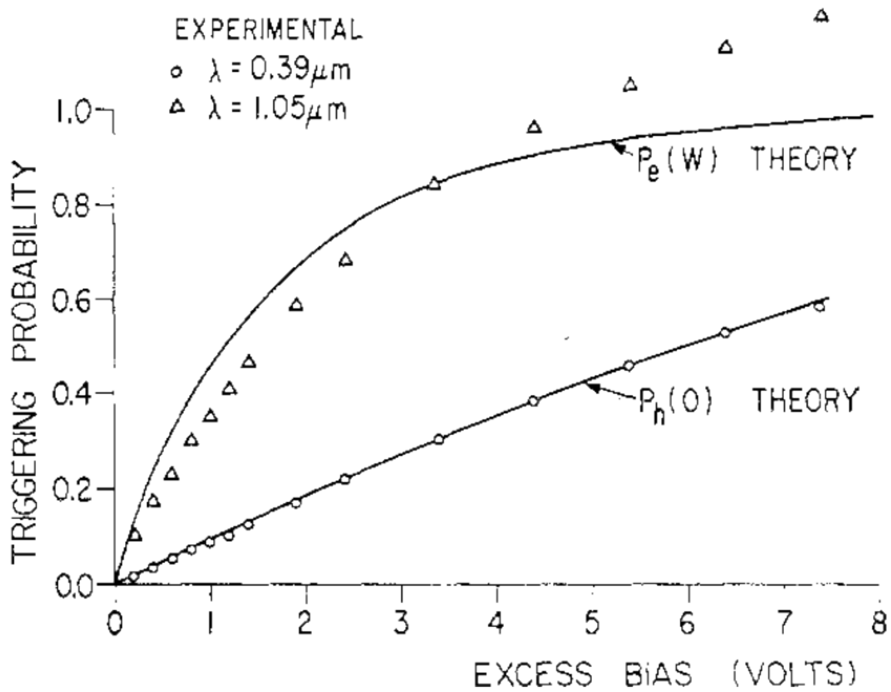

- avalanche can be started by electrons or holes, depending on λ and location of pair creation
- ionization rate is larger for electrons, those are more likely to trigger an avalanche

Optical Cross Talk I

R. Newman, PR100, 1955, 700

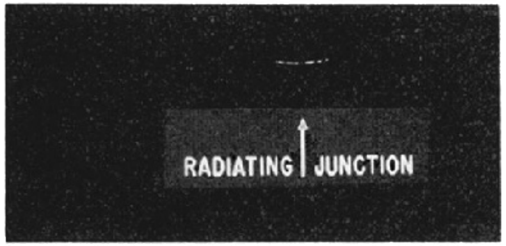

FIG. 1. A photograph of the light emitted from a worked silicon *p-n* junction unit operating in the breakdown region. The junction is the horizontal bow-shaped curve. Current flows vertically across it.

- photons from visible and infrared spectrum can be emitted during breakdown in a cell

  → can trigger breakdowns in neighbouring cells
- remedied by trenches between cells (→ limits fill factor)

R. Mirzoyan, NDIP08, Aix-les-Bains

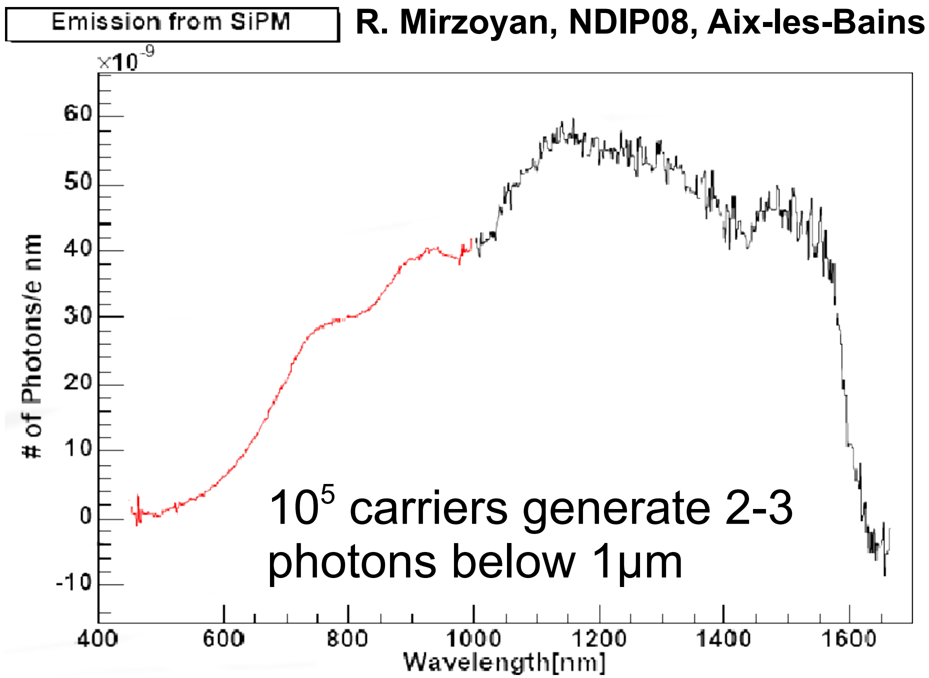

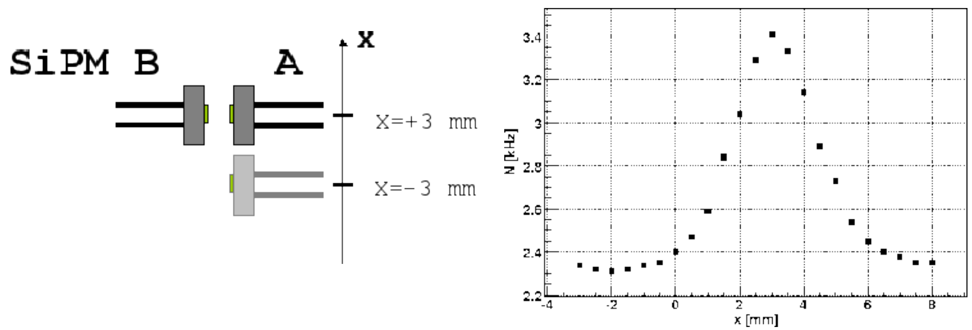

H. Chagani et al., NP B197 (2009) 283

Optical Cross Talk II

M. Lauscher, RWTH Aachen

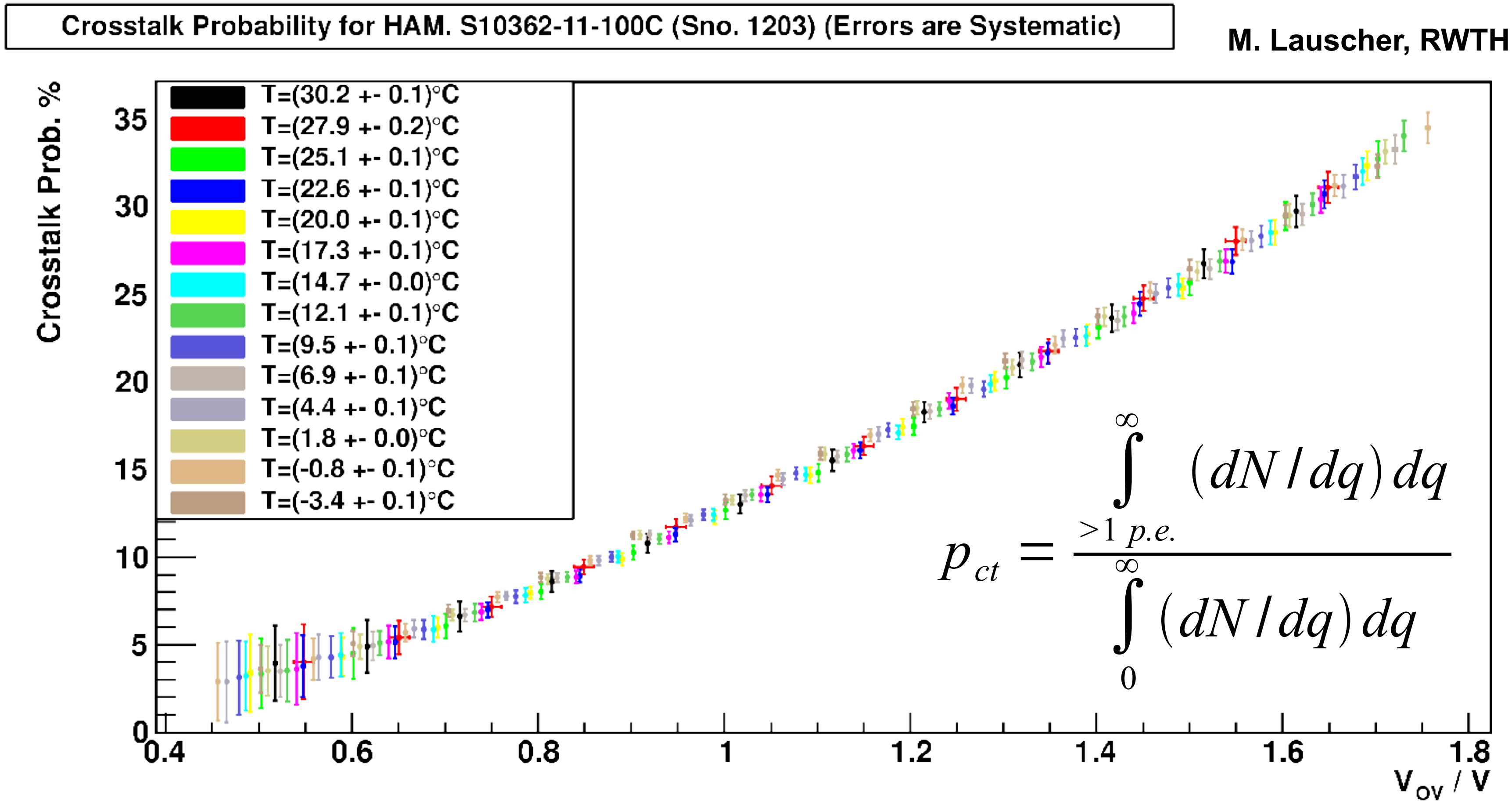

$$p_{ct} = \frac{\int_{>1\ p.e.}^{\infty} (dN/dq)\,dq}{\int_{0}^{\infty} (dN/dq)\,dq}$$

- derive cross talk probability from QDC spectrum
- cross talk independent on temperature (at proper overvoltage)

Afterpulsing I

- carriers can be trapped during avalanche breakdown and released later on

  → can trigger a new avalanche several 100ns afterwards
- increase the noise for large charge integration windows

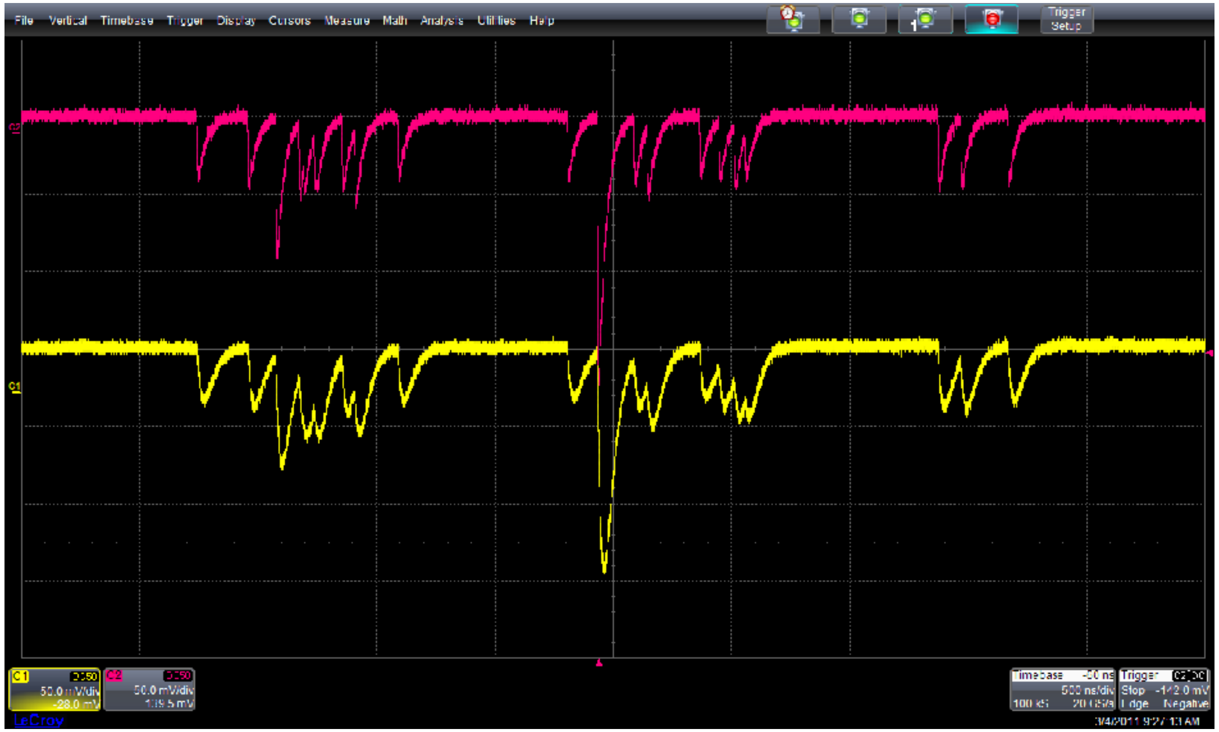

Afterpulsing II

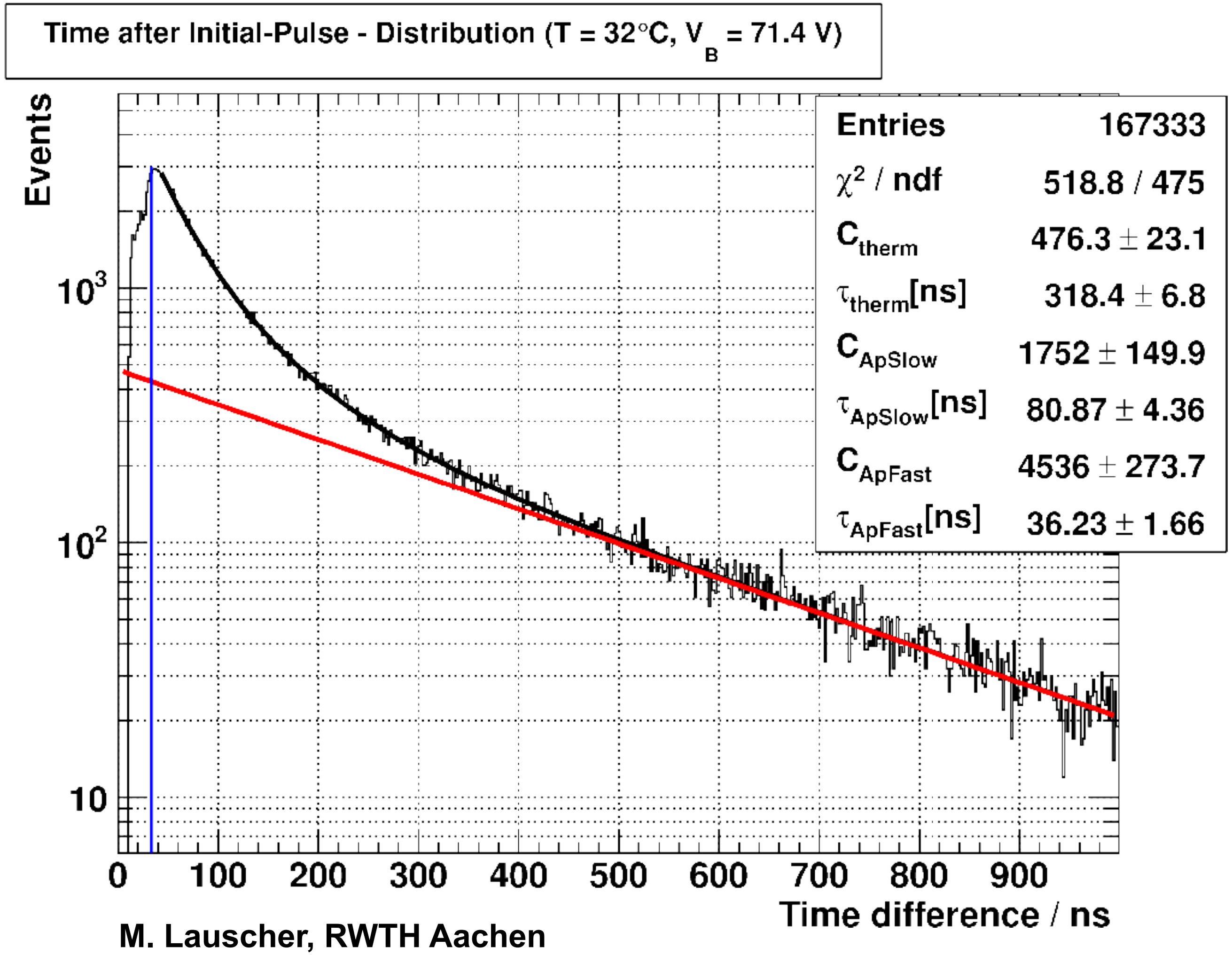

- evaluate time difference between successive peaks
- request 'quiet' time interval of 300ns before trigger pulse
- various components
  - 'dead time' effects
  - thermal contributions (~3MHz)
  - fast and slow afterpulsing effects

Dynamic Range / Recovery Time

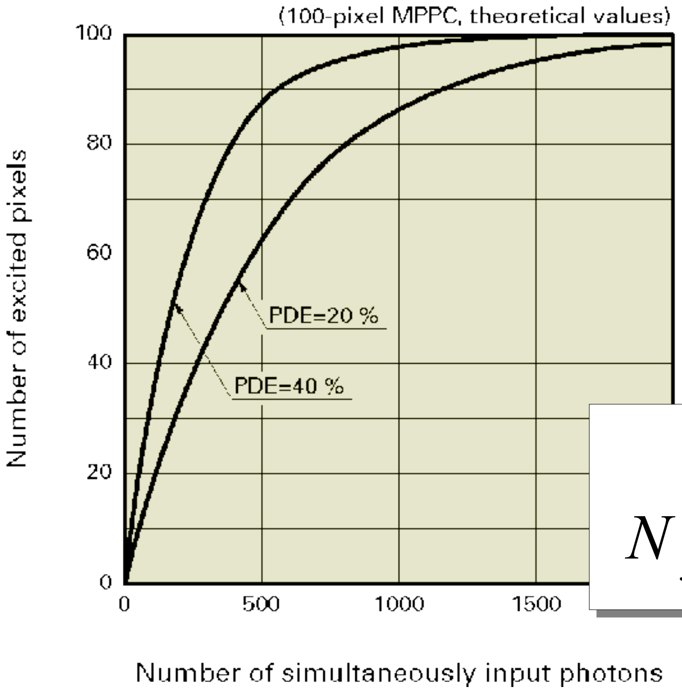

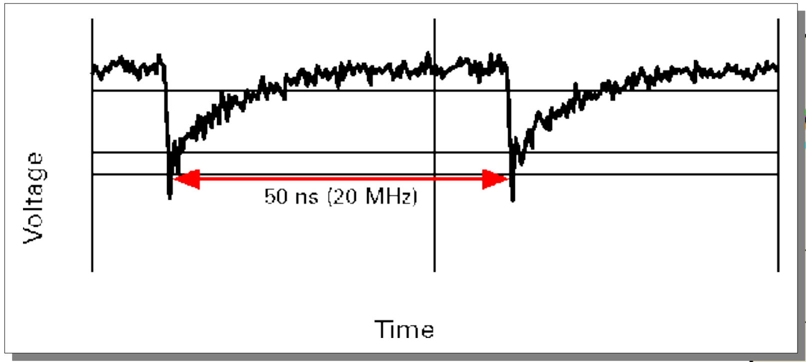

$$N_{fired} = N_{cell} \cdot \left(1 - e^{-\eta \frac{N_{ph}}{N_{pixel}}}\right)$$

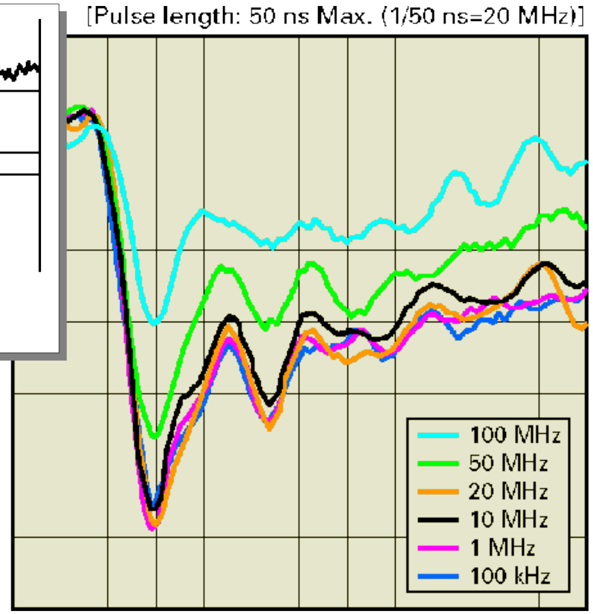

Hamamatsu Photonics

- number of cells determines dynamic range
- good linearity only for $N_\gamma << N_{cell}$
- valid for ideal SiPM...

- fired cells need time to fully recover ($V_{bd} \rightarrow V_{op}$)
  - ~ 20 to 200 ns for pixel sizes from 25 to 100 μm
- dd

Summary Part IV

- SiPM operation requires fine control of the operating conditions – it is very sensitive to even small changes of operating voltage (overvoltage) and ambient temperature
- SiPM is 'a collection' of diodes and series resistors → well known I-V characteristics and features (breakdown voltage, diffusion voltage, ohmic behaviour, dark current)
- SiPM output: discrete pulses – integrated yields a 'finger spectrum' → count photons
- SiPMs have a high dark count rate which can be controlled by V_{op} and T but requires the application of thresholds for noise reduction
- the photodetection efficiency depends on the material properties, the cell geometry and the operating conditions (overvoltage, T)
- phenomena like afterpulsing and optical cross talk produce a substantial noise of the device (w.r.t. thermal noise)

V. Special Topics

SiPM Quenching Mechanism

- detailed numerical simulation of the avalanche process
- during avalanche capacitance voltage of depletion layer decreases
- avalanche stops when the voltage drops below the breakdown voltage

  → avalanche is first quenched by the discharge of the diode capacity

  → current quenching resistors are too large and result in long recovery times

V.N. Grebenyuk et al., arxiv:0903.1161

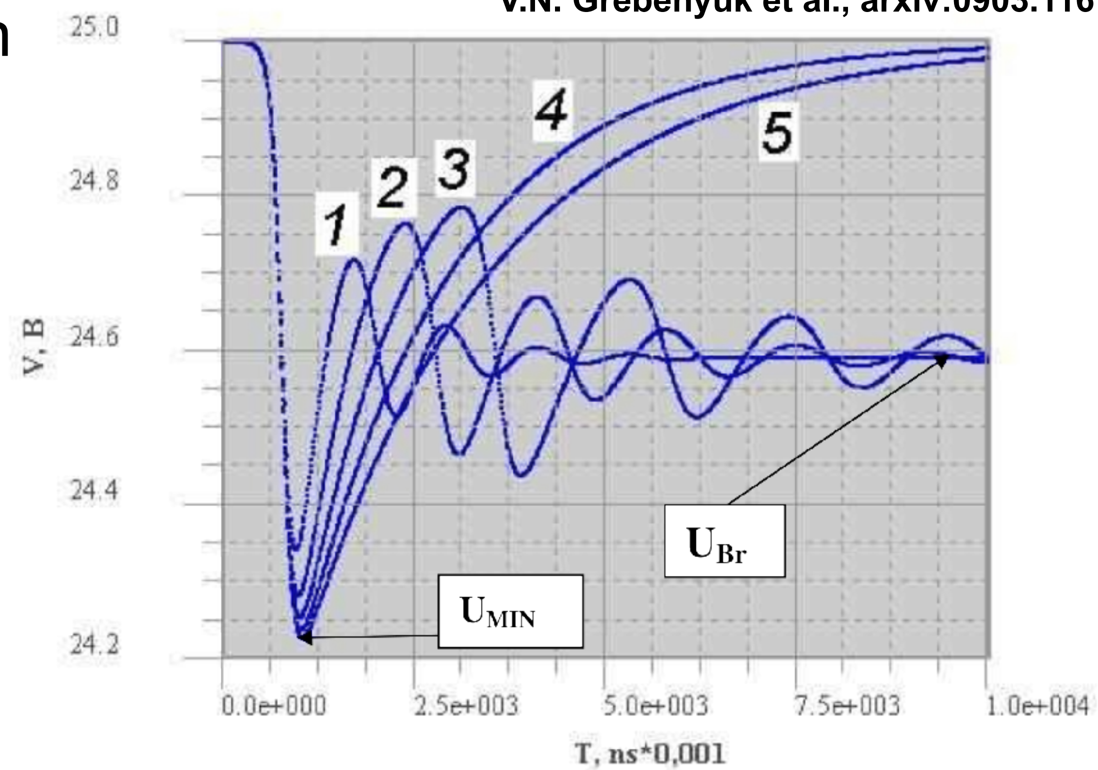

Fig. 1. Photodiode voltage V as a function of time at the operation voltage E_{OV}=25 V and diode capacitance 0.25 pF for R_q =2, 4, 6, 8, and 10 kΩ, labeled by numbers 1, 2, 3, 4, and 5 respectively. U_{br} is the threshold voltage.

Electrical Model of an SiPM

F. Corsi,
NIM A572 (2007) 416

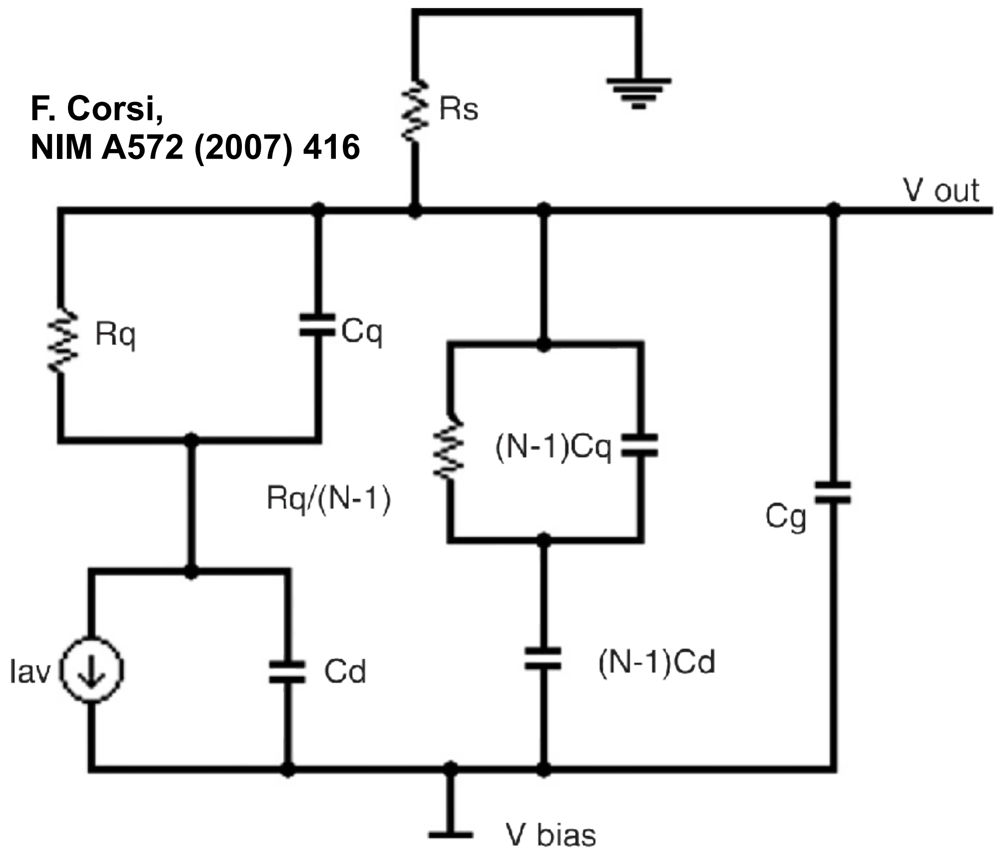

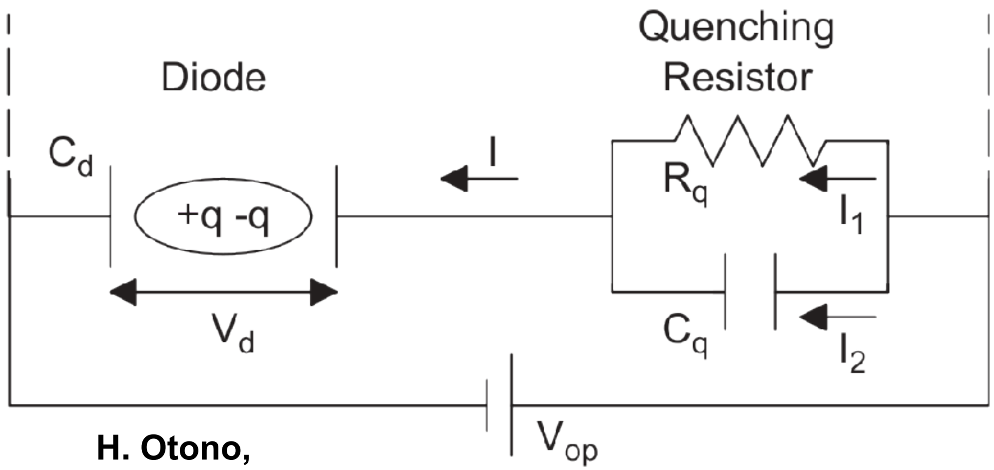

H. Otono,
NIM A610 (2009) 397

- model includes generation of carriers by avalanche process → time dependence of multiplied photocurrent
- dedicated waveform analysis for dead time determination

- model of one active pixel plus (N-1) 'silent' pixels

$$Q=(C_d+C_q)\Delta V$$

Summary

- building a good SiPM requires a lot of 'fine tuning' and a lot of knowledge about solid state physics ('which particle physicists mostly try to avoid...')
- SiPM exhibits all facets of a silicon photodetector → nice toy
- SiPMs nowadays are used in certain niches (where the noise is not a big issue)
- large-scale usage in HEP experiments is starting now but still requires a lot of R&D and testing

Outlook

- we will see various SiPMs for special needs (low noise, timing properties, UV-enhanced, high dynamic range, high PDE, digital SiPMs, ...)
  - medical physics
  - astroparticle physics
  - HEP experiments
  - (…and whatever else they can be used for...)